Original

Evaluation of the Subchronic Toxicity of Dietary Administered *Equisetum arvense* in F344 Rats

Yoshiyuki Tago[1], Min Wei[1], Naomi Ishii[1], Anna Kakehashi[1], and Hideki Wanibuchi[1]

[1]Department of Pathology, Osaka City University Medical School, 1-4-3 Asahi-machi, Abeno-ku, Osaka 545-8585, Japan

Abstract: *Equisetum arvense*, commonly known as the field horsetail, has potential as a new functional food ingredient. However, little information is available on its side effects, and the general toxicity of *Equisetum arvense* has yet to be examined in detail. In the present study, we evaluated the influence of administration in diet at doses of 0, 0.3, 1 and 3% for 13 weeks in male and female F344 rats. No toxicity was detected with reference to clinical signs, body weight, urinalysis, hematology and serum biochemistry data and organ weights. Microscopic examination revealed no histopathological lesions associated with treatment. In conclusion, the no-observed-adverse-effect level (NOAEL) for *Equisetum arvense* was determined to be greater than 3% in both sexes of F344 rat (males and females: >1.79 g/kg BW/day and >1.85 g/kg BW/day, respectively) under the conditions of the present study. (J Toxicol Pathol 2010; 23: 245–251)

Key words: *Equisetum arvense*, horsetail, NOAEL, toxicity, F344 rat

Introduction

Equisetum arvense, commonly known as the field horsetail, is a bushy perennial featuring rhizomatous stem formation[1]. The plant contains abundant minerals such as silicon and calcium[2], as well as small amounts of pharmacologically active compounds, and has been used as a traditional medicine to stop bleeding, heal ulcers and wounds and treat tuberculosis and kidney diseases. It is available as a dried extract in powdered form or a liquid extract, and its biological effects include anti-oxidant[3, 4], anti-convulsant and sedative actions[5], as demonstrated in recent *in vitro* and *in vivo* studies. In particular, it is expected to lower high blood pressure due to its diuretic effect, which was previously observed in rats and humans[6]. Therefore, *Equisetum arvense* may have potential as new functional food ingredient.

Recently, no genetic toxicity of *Equisetum arvense* was reported in a reverse mutation test, chromosomal aberration test or micronucleus test[7]. Additionally, the LD$_{50}$ value of *Equisetum arvense* was found to exceed 5000 mg/kg in a single-dose toxicity study in rats[7].

However, it was reported to cause skin dermatitis in people allergic to tobacco smoke[8]. Furthermore, little is known about its side effects when continuously administered via the oral route.

In the present study, we therefore examined the general toxicity of *Equisetum arvense* administered in diet for 13 weeks to male and female F344 rats.

Materials and Methods

Animals and test chemical

Five-week-old F344 rats (40 males and 40 females) were obtained from Charles River Laboratories Japan, Inc. (Kanagawa, Japan) and housed in a room maintained under a 12-h light/dark cycle at constant temperature (23 ± 1°C) and humidity (50 ± 5%). Test chemicals (Lot.183-3194G, Cross Co., Ltd., Osaka, Japan), a yellow-green to yellow fresh powder, were prepared every month from *Equisetum arvense*, extracted with hot water and mixed with powdered CRF-1 basal diet (Oriental Yeast, Tokyo, Japan) at each concentration. The diet of each group was changed twice a week during the experiment.

Experimental design

All procedures were approved by the Institutional Animal Care and Use Committee of Osaka City University Medical School. After acclimation for 1 week, male and female rats at six weeks of age were randomly divided into eight groups of 10 rats each. Dosage selections were based on estimated intake for humans as follows. We expected that people consumed 5 mg/kg *Equisetum arvense* daily as a sup-

Table 1. Intake of *Equisetum arvense* during the Experiment

	Food consumption (g/rat/day)		Intake of *Equisetum arvense* (g/rat/day)		(g/kg BW/day)		Total intake of *Equisetum arvense* (g/rat)	
	Male	Female	Male	Female	Male	Female	Male	Female
0%	13.4	8.6	–	–	–	–	–	–
0.3%	14.0	8.5	0.04	0.03	0.18	0.17	3.78	2.30
1%	13.6	8.8	0.14	0.09	0.59	0.60	12.28	7.94
3%	13.5	9.0	0.40	0.27	1.79	1.85	36.44	24.17

plement. To ensure a safety factor of 100-fold, the 1% dose was set to feed at an approximate dosage level of 500 mg/kg, and 3 and 0.3% doses were chosen as the high and low dose groups using a common ratio of about 3. The animals received diets containing *Equisetum arvense* at doses of 0, 0.3, 1 and 3%, respectively, for 13 weeks. They were observed daily for clinical signs and mortality. Body weight and food consumption were measured weekly. Fresh urine samples were collected from all animals at week 13. Urinalysis using N-multistix SG-L and Clinitek Status (Siemens, Tokyo, Japan) was performed for the following parameters: glucose (GLU), bilirubin (BIL), ketone (KET), specific gravity (SG), protein (PRO), urobilinogen (URO), occult blood (OB), pH and nitrite (NIT). At the end of the experiment, all animals were fasted overnight and euthanized by exsanguination under ether anesthesia. Blood was taken from the abdominal aorta for hematology and serum biochemistry analyses. Hematological examinations included the following parameters: white blood cell count (WBC), red blood cell count (RBC), hemoglobin concentration (Hb), hematocrit (Ht), platelet count (PLT), mean corpuscular volume (MCV), mean corpuscular hemoglobin (MCH) and mean corpuscular hemoglobin concentration (MCHC). Serum biochemistry was performed to examine total proteins (TP), albumin (ALB), albumin/globulin ratio (A/G), aspartate aminotransferase (AST), alanine aminotransferase (ALT), alkaline phosphatase (ALP), gamma glutamyl transpeptidase (γ-GTP), creatinine (CRN), triglycerides (TG), total cholesterol (T-Cho), total bilirubin (T-Bil), blood urea nitrogen (BUN), sodium (Na), potassium (K), chloride (Cl), calcium (Ca) and inorganic phosphorus (P). Analyses for hematology and serum biochemistry were conducted at Mitsubishi Chemical Medience Corp., (Osaka, Japan) using automatic analyzing machines, XT-2100 (Sysmex, Hyogo, Japan) and H7700 (Hitachi, Tokyo, Japan), for blood and serum analyses, respectively. At sacrifice, the heart, liver, spleen, kidneys, adrenals, testes, brain and thymus were excised and weighed. In addition to these organs, the lymph nodes (cervical and mesenteric), aorta, salivary gland, bone (sternum, femur), bone marrow, trachea, thyroid, tongue, esophagus, stomach, duodenum, small intestine, large intestine, pancreas, urinary bladder, seminal vesicles, prostate gland, epididymis, ovaries, uterus, vagina, pituitary gland, sciatic nerve, skeletal muscle, spinal cord, eyes and harderian glands were excised and fixed in 10% buffered formalin.

Testes were fixed in Bouin's solution. Paraffin-embedded tissue sections of all organs and tissues were routinely prepared and stained with hematoxylin and eosin for histopathological examination. All organs and tissues in the control and high-dose groups were examined. Histopathological examination was also extended to all tissues of the low- and medium-dose groups if lesions were frequently found in the high-dose group.

Immunohistochemistry

The avidin-biotin complex (ABC) method was used to demonstrate alpha2u-globulin expression in the kidney. After deparaffinization, kidney sections were treated in a microwave oven sequentially with 3% H_2O_2, normal rabbit serum, goat polyclonal anti- alpha2u-globulin antibody (AF586, R&D Systems, Inc., Minneapolis, MN, USA) diluted 1:300, biotin-labeled secondary antibody and avidin-biotin complex (Vectastain ABC kit, Funakoshi, Tokyo, Japan). Tissue sections were lightly counterstained with hematoxylin. Kidney tissue sections without addition of primary antibody were used as negative controls. For positive controls, kidneys of rats administered $KBrO_3$, which is known to increase alpha2u-globulin, were subjected to analysis.

Statistics

The Dunnett's multiple range test was employed for comparison of body weights, urinalysis, organ weights (both absolute and relative), hematology and serum biochemistry data between the control and treated groups. For all comparisons, p-values less than 0.05 were considered to be statistically significant (Stat Light, Yukms Co., Ltd., Tokyo, Japan).

Results

Clinical observations and survival

No deaths or obvious clinical signs were noted in any of the animals throughout the experimental period. During the experiment, the body weights and cumulative body weight gains in all treatment groups were similar to those of the controls (Fig. 1). The total intake of *Equisetum arvense* (g/rat) for 13 weeks was 0 (0%), 3.8 (0.3%), 12.3 (1%) and 36.4 (3%) in males and 0 (0%), 2.3 (0.3%), 7.9 (1%) and 24.2 (3%) in females (Table 1). There was no difference in food consumption.
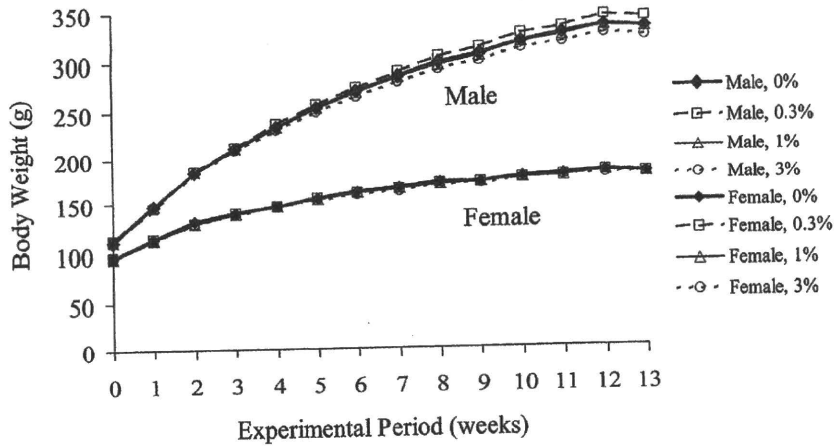
Fig. 1. Body weight changes in F344 rats given *Equisetum arvense*. Symbols represent the means.
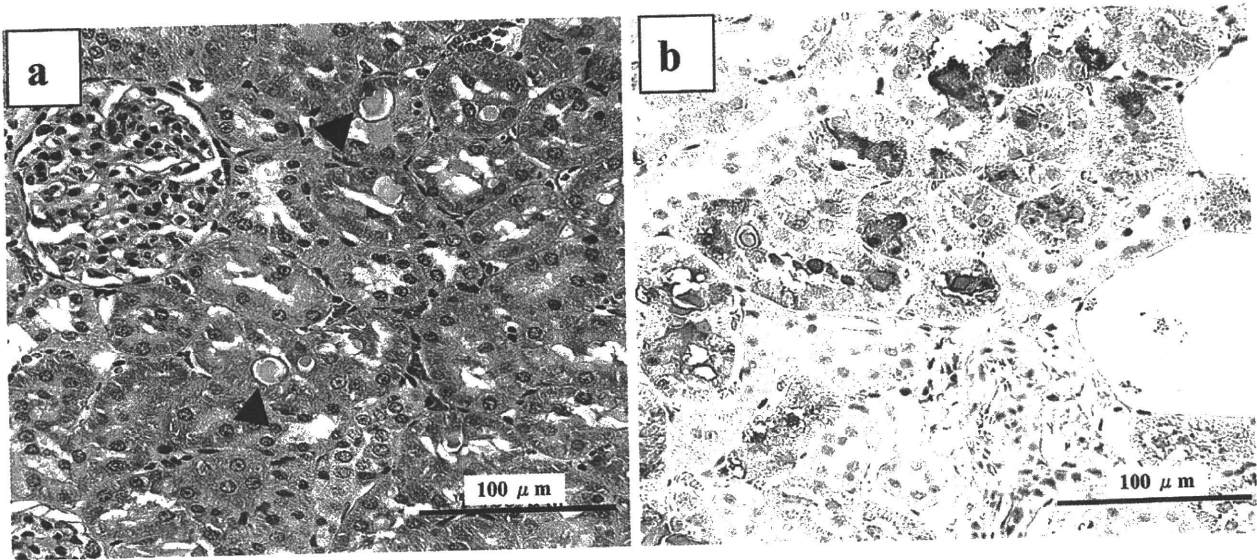

Fig. 2. Eosinophilic body with overexpression of alpha2u-globulin in the rat kidney. Kidney sections from male control rats were used to confirm whether eosinophilic bodies (arrowheads) were also positive for alpha2u-globulin. Some epithelial cells in proximal tubules were positive. a: HE stain. b: immunohistochemistry for alpha2u-globulin. Scale bar shows 100 μm.
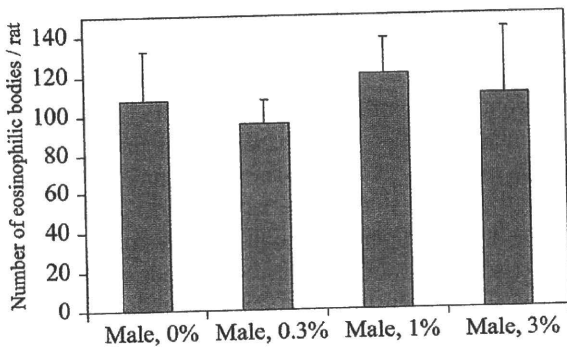

Fig. 3. Number of eosinophilic bodies in male rat kidneys. No significant differences were observed among the groups. The column and whisker represent the mean and standard deviation, respectively.

Urinalysis

There were no significant differences in any of the parameters among the groups, but the protein levels in the 1 and 3% male groups tended to decrease (Table 2).

Hematology and serum biochemistry

Significant alterations were observed in hematological parameters (Table 3), including increased MCH in the 0.3% males, increased PLT in the 1% females and decreased MCH in the 1% females ($p<0.05$), but no dose dependence was apparent. In addition, a trend towards a dose-dependent decrease in WBC was found in the females. Data for serum biochemistry are shown in Table 4. There were significant decreases in Ca in the 1 and 3% male groups ($p<0.01$ and $p<0.05$) and in T-Cho in the 3% males ($p<0.05$). A trend

Table 2. Urinalysis Data for F344 Rats Given *Equisetum arvense*

Sex	Dose (%)	No. of rats	KET					SG				URO		GLU	PRO (mg/dl)			
			−	±	1+	2+	3+	1.015	1.020	1.025	1.030	0.1	1.0	−	−	±	30	100
Male	0	10	0	1	3	6	0	2	7	1	0	6	4	10	0	1	1	8
	0.3	10	0	0	1	7	2	2	5	3	0	7	3	10	0	0	3	7
	1	10	0	0	5	5	0	3	7	0	0	9	1	10	1	0	7	2
	3	10	0	0	2	8	0	1	7	2	0	7	3	10	0	0	7	3
Female	0	10	1	9	0	0	0	2	6	2	0	7	3	10	0	5	5	0
	0.3	10	3	5	2	0	0	6	4	0	0	8	2	10	2	2	5	1
	1	10	2	6	2	0	0	5	3	1	1	10	0	10	0	4	6	0
	3	10	3	6	1	0	0	3	5	2	0	8	2	10	2	5	3	0

Sex	Dose (%)	No. of rats	pH					OB				NIT		BIL	
			6.5	7.0	7.5	8.0	8.5	−	±	1+	2+	−	+	−	+
Male	0	10	0	0	0	0	10	5	5	0	0	10	0	6	4
	0.3	10	0	0	1	0	9	7	1	2	0	10	0	7	3
	1	10	0	0	1	1	·8	6	3	1	0	9	1	9	1
	3	10	0	0	0	0	10	8	1	0	1	9	1	6	4
Female	0	10	0	0	0	0	10	10	0	0	0	10	0	5	5
	0.3	10	0	0	0	0	10	9	1	0	0	10	0	9	1
	1	10	1	0	1	1	7	10	0	0	0	10	0	6	4
	3	10	0	0	3	0	7	8	2	0	0	10	0	7	3

Data show the numbers of rats for each value per parameter. Ketone (KET), specific gravity (SG), urobilinogen (URO), glucose (GLU), protein (PRO), occult blood (OB), nitrite (NIH), bilirubin (BIL).

Table 3. Hematological Data for F344 Rats Given *Equisetum arvense*

Sex	Dose (%)	No. of rats	RBC (×10⁴/μL)	Hb (g/dL)	Ht (%)	MCV (fL)	MCH (pg)	MCHC (%)	PLT (×10⁴/μL)	WBC (/μL)
Male	0	10	894 ± 22	14.8 ± 0.5	47.6 ± 1.5	53.3 ± 0.9	16.5 ± 0.2	31.1 ± 0.4	55.9 ± 3.7	3460 ± 707
	0.3	10	895 ± 17	15.0 ± 0.3	47.3 ± 0.8	52.9 ± 0.6	16.8 ± 0.2*	31.7 ± 0.4	54.9 ± 2.4	3650 ± 366
	1	10	902 ± 26	14.9 ± 0.4	47.6 ± 1.0	52.7 ± 0.8	16.6 ± 0.1	31.4 ± 0.5	57.2 ± 3.4	3640 ± 881
	3	10	901 ± 23	4.8 ± 0.4	47.2 ± 0.9	52.5 ± 1.1	16.5 ± 0.4	31.4 ± 0.8	53.1 ± 7.4	3460 ± 1237
Female	0	10	821 ± 21	15.1 ± 0.5	46.6 ± 1.7	56.8 ± 1.8	18.4 ± 0.5	32.3 ± 0.6	50.4 ± 7.4	3300 ± 1083
	0.3	10	842 ± 21	15.4 ± 0.4	47.7 ± 1.3	56.7 ± 0.7	18.3 ± 0.1	32.4 ± 0.4	55.9 ± 4.5	3140 ± 986
	1	10	835 ± 20	14.9 ± 0.3	46.2 ± 1.1	55.3 ± 0.9	17.9 ± 0.3*	32.3 ± 0.8	57.0 ± 4.3*	2970 ± 525
	3	10	832 ± 35	14.9 ± 0.5	47.1 ± 2.2	56.4 ± 1.3	17.9 ± 0.4	31.6 ± 0.9	55.6 ± 5.0	2780 ± 627

Data are presented as the means ± standard deviations. * Significantly different from the control (0%) group ($p<0.05$). Red blood cell count (RBC), hemoglobin concentration (Hb), hematocrit (Ht), mean corpuscular volume (MCV), mean corpuscular hemoglobin (MCH), mean corpuscular hemoglobin concentration (MCHC), platelet count (PLT), white blood cell count (WBC).

towards a dose-dependent decrease in TG was found in the males.

Organ weights

Absolute and relative organ weights are summarized in Table 5. There were no significant differences in any organ weights. A tendency towards a decrease in the absolute weights of the adrenals was observed in the males.

Macroscopic and microscopic findings

No treatment-related macroscopic changes were observed in any of the animals at sacrifice. Histopathologi-

cally, spontaneous inflammatory and proliferative lesions in the liver and pancreas, microgranulomas in the liver, atrophy in kidneys and cysts in the ovary and pituitary glands were diagnosed. All the changes were of minimal grade. Eosinophilic bodies and alpha2u-globulin expression in the proximal tubules of the kidneys were observed in all male rats, including the 0% group (Fig. 2). Extended microscopic examination of kidneys in the 0.3 and 1% male groups showed no histopathological changes compared with the 0% group (Table 6). The number of eosinophilic bodies per rat among the groups was not significantly different (Fig. 3). Moreover, no treatment-related findings were revealed in

Table 4. Serum Biochemistry Results for F344 Rats given *Equisetum arvense*

Sex	Dose (%)	No. of rats	TP (g/dL)	A/G	ALB (g/dL)	T-Bil (mg/dL)	T-Cho (mg/dL)	TG (mg/dL)	BUN (mg/dL)	CRN (mg/dL)	γ-GTP (IU/L)
Male	0	10	6.4 ± 0.1	2.4 ± 0.1	4.5 ± 0.1	0.1 ± 0	72 ± 6	91 ± 19	25 ± 4	0.30 ± 0.04	1.1 ± 0.3
	0.3	10	6.4 ± 0.1	2.4 ± 0.1	4.5 ± 0.1	0.1 ± 0	71 ± 2	88 ± 20	25 ± 4	0.29 ± 0.02	1.3 ± 0.5
	1	10	6.4 ± 0.2	2.4 ± 0.1	4.5 ± 0.1	0.1 ± 0	69 ± 4	85 ± 17	25 ± 4	0.29 ± 0.03	1.2 ± 0.6
	3	10	6.4 ± 0.3	2.4 ± 0.2	4.5 ± 0.1	0.1 ± 0	65 ± 5*	81 ± 13	24 ± 5	0.28 ± 0.03	1.4 ± 1.0
Female	0	10	6.3 ± 0.1	2.8 ± 0.3	4.6 ± 0.2	0.1 ± 0	88 ± 6	50 ± 13	24 ± 5	0.29 ± 0.03	1.3 ± 0.5
	0.3	10	6.2 ± 0.2	2.8 ± 0.2	4.6 ± 0.1	0.1 ± 0	92 ± 5	56 ± 19	23 ± 6	0.30 ± 0.03	1.1 ± 0.6
	1	10	6.2 ± 0.2	2.8 ± 0.2	4.6 ± 0.1	0.1 ± 0	87 ± 7	39 ± 16	23 ± 7	0.28 ± 0.02	1.1 ± 0.3
	3	10	6.1 ± 0.1	2.8 ± 0.2	4.5 ± 0.1	0.1 ± 0	85 ± 7	48 ± 12	23 ± 4	0.29 ± 0.03	1.0 ± 0.6

Sex	Dose (%)	No. of rats	P (mg/dL)	Na (mEq/L)	Cl (mEq/L)	K (mEq/L)	Ca (mg/dL)	AST (IU/L)	ALT (IU/L)	ALP (IU/L)
Male	0	10	6.1 ± 0.4	146 ± 1	101 ± 1	4.3 ± 0.2	10.5 ± 0.2	130 ± 25	71 ± 7	461 ± 56
	0.3	10	6.2 ± 0.5	146 ± 1	101 ± 1	4.4 ± 0.2	10.4 ± 0.3	145 ± 31	74 ± 11	470 ± 50
	1	10	6.2 ± 0.5	146 ± 1	100 ± 1	4.4 ± 0.3	10.1 ± 0.1*	130 ± 19	66 ± 6	481 ± 50
	3	10	6.5 ± 0.5	145 ± 1	100 ± 2	4.6 ± 0.5	10.2 ± 0.2*	143 ± 52	72 ± 10	462 ± 34
Female	0	10	4.8 ± 0.8	144 ± 1	102 ± 1	4.3 ± 0.4	9.8 ± 0.2	104 ± 11	43 ± 6	324 ± 47
	0.3	10	4.9 ± 0.7	144 ± 2	102 ± 1	4.3 ± 0.4	9.8 ± 0.2	103 ± 12	42 ± 5	324 ± 66
	1	10	4.8 ± 0.6	144 ± 1	102 ± 1	4.3 ± 0.3	9.6 ± 0.2	104 ± 8	42 ± 6	295 ± 51
	3	10	5.0 ± 1.2	144 ± 1	102 ± 1	4.7 ± 0.8	9.8 ± 0.2	100 ± 12	42 ± 6	314 ± 40

Data are presented as mean ± SD. * Significantly different from the control (0%) group ($p<0.05$). Total proteins (TP), albumin/globulin ratio (A/G), albumin (ALB), total bilirubin (T-Bil), total cholesterol (T-Cho), triglycerides (TG), blood urea nitrogen (BUN), creatinine (CRN), gamma glutamyl transpeptidase (γ-GTP), inorganic phosphorus (P), sodium (Na), chloride (Cl), potassium (K), calcium (Ca), aspartate aminotransferase (AST), alanine aminotransferase (ALT), alkaline phosphatase (ALP).

Table 5. Organ Weights of F344 Rats Given *Equisetum arvense*

Sex	Dose (%)	No. of rats	Heart (g)	Liver (g)	Kidneys (g)	Thymus (g)
Male	0	10	0.93 ± 0.05 (0.28)	7.34 ± 0.57 (2.24)	1.83 ± 0.17 (0.56)	0.24 ± 0.07 (0.07)
	0.3	10	0.96 ± 0.05 (0.29)	7.72 ± 0.60 (2.29)	1.97 ± 0.12 (0.58)	0.27 ± 0.10 (0.08)
	1	10	0.94 ± 0.06 (0.29)	7.36 ± 0.45 (2.26)	1.89 ± 0.10 (0.58)	0.21 ± 0.05 (0.06)
	3	10	0.89 ± 0.06 (0.28)	7.03 ± 0.48 (2.22)	1.81 ± 0.05 (0.57)	0.21 ± 0.06 (0.07)
Female	0	10	0.59 ± 0.03 (0.33)	3.75 ± 0.23 (2.12)	1.13 ± 0.10 (0.64)	0.17 ± 0.03 (0.10)
	0.3	10	0.59 ± 0.04 (0.34)	3.74 ± 0.17 (2.11)	1.14 ± 0.07 (0.64)	0.18 ± 0.03 (0.10)
	1	10	0.59 ± 0.05 (0.34)	3.71 ± 0.23 (2.09)	1.14 ± 0.09 (0.64)	0.18 ± 0.04 (0.10)
	3	10	0.60 ± 0.04 (0.34)	3.83 ± 0.39 (2.18)	1.17 ± 0.07 (0.67)	0.17 ± 0.02 (0.10)

Sex	Dose (%)	No. of rats	Brain (g)	Adrenals (g)	Spleen (g)	Testes (g)
Male	0	10	1.97 ± 0.07 (0.60)	0.043 ± 0.012 (0.013)	0.66 ± 0.04 (0.20)	3.10 ± 0.16 (0.95)
	0.3	10	1.97 ± 0.07 (0.58)	0.040 ± 0.007 (0.012)	0.65 ± 0.03 (0.19)	3.07 ± 0.12 (0.91)
	1	10	1.99 ± 0.03 (0.61)	0.039 ± 0.012 (0.012)	0.63 ± 0.03 (0.19)	3.03 ± 0.17 (0.93)
	3	10	1.96 ± 0.04 (0.62)	0.034 ± 0.007 (0.011)	0.63 ± 0.03 (0.20)	3.06 ± 0.11 (0.97)
Female	0	10	1.81 ± 0.04 (1.03)	0.041 ± 0.007 (0.023)	0.40 ± 0.02 (0.23)	—
	0.3	10	1.80 ± 0.06 (1.02)	0.041 ± 0.006 (0.023)	0.40 ± 0.02 (0.23)	—
	1	10	1.83 ± 0.06 (1.04)	0.039 ± 0.008 (0.022)	0.40 ± 0.04 (0.23)	—
	3	10	1.80 ± 0.04 (1.03)	0.040 ± 0.004 (0.023)	0.41 ± 0.06 (0.23)	—

Data are presented as the means ± standard deviations. Values in parentheses show the mean relative organ weights.

Table 6. Histopathological Findings for F344 Rats Given *Equisetum arvense*

Organ/Finding Dose(%)	Male				Female			
	0	0.3	1	3	0	0.3	1	3
Liver	(10)	–	–	(10)	(10)	–	–	(10)
Microgranuloma	1	–	–	1	1	–	–	2
Inflammatory cell infiltration	1	–	–	1	0	–	–	0
Proliferation, bile duct	1	–	–	1	0	–	–	0
Kidney	(10)	(10)	(10)	(10)	(10)	(10)	(10)	(10)
Eosinophilic body	10	10	10	10	0	0	0	0
Regeneration, proximal tubule	3	3	2	1	0	0	0	1
Pancreas	(10)	–	–	(10)	(10)	–	–	(10)
Inflammatory cell infiltration	1	–	–	0	0	--	–	0
Proliferation, pancreatic duct	0	–	–	0	0	–	–	1
Ovary	–	–	–	–	(10)	(1)	–	(10)
Cyst					0	1		0
Pituitary	(10)	–	–	(10)	(10)	–	–	(10)
Cyst	1	–	–	0	0	–	–	0

Data show the numbers of rats observed with each lesion. Values in parentheses show the examined number of rats.

other tissues and organs of the male or female rats.

Discussion

In the present study, dietary administration with *Equisetum arvense* for 13 weeks was not found to alter body weight in either gender of rat. The decline of the urine protein levels after administration of *Equisetum arvense* in the 1 and 3% male groups may be related to its diuretic effect, which was previously reported[6]. Although the WBC in females and the weights of the adrenals in males were dose-dependently decreased, no histopathological changes related to inflammation and atrophy of adrenals were observed. Furthermore, although a significant decrease in the concentration of serum Ca was noted in the 1 and 3% groups in males, all values were within the physiological range previously observed in our lab. A significant decrease in T-Cho and a tendency for decrease in TG were seen in a dose-related manner in males, but no histopathological changes pointing to altered lipid metabolism were observed in the liver.

Histopathological examination of kidneys revealed the existence of intracytoplasmic granules, diagnosed as eosinophilic bodies, seen in the proximal tubules in all male groups (Fig. 2a), but not in the female rats. These granules were demonstrated to be alpha2u-globulin by immunohistochemistry (Fig. 2b). Abnormal accumulation of alpha2u-globulin is known to be related to nephropathy and renal carcinogenesis in male rats[9, 10]. As no difference in the number of eosinophilic bodies was seen between the control and treated groups, administration of *Equisetum arvense* clearly exerted no effects on the formation of alpha2u-globulin.

In an earlier toxicological report for rats[11], dietary administration of 4% *Equisetum arvense* with 0.5% cholesterol and 0.15% sodium cholate for 14 days caused dermatitis of the neck, head and back skin in about 20-65%

of rats, with no significant differences in the serum IgE levels. However, clinical signs, such as redness and edema, were not observed in this 13-week dietary administration study. Therefore, it is likely that *Equisetum arvense* alone does not induce dermatitis in rats and that the changes observed in the earlier study were probably due to coadministration of excess amounts of cholesterol and/or sodium cholate with *Equisetum arvense*[11].

In humans, it was reported that seborrhoeic dermatitis occurred in some patients, transdermal absorption of *Equisetum arvense* after passive inhalation of tobacco smoke[8]. Smoke components, such as nicotine and formaldehyde are considered to cause allergic contact dermatitis[12].

However, the results of the present study showed no adverse effects of *Equisetum arvense* when administered alone in diet. Taking into accounts these reports, we predict that additional factors such as a potential allergen of tobacco might influence the side effects of *Equisetum arvense*.

In conclusion, we determined the no-observed-adverse-effect level (NOAEL) for *Equisetum arvense* to be more than 3% in both male and female rats (males and females: >1.79 g/kg BW/day and >1.85 g/kg BW/day, respectively) under the conditions of the present study.

References

1. Nijole B, Valentinas S, and Steponas C. The spread of field horsetail (*Equisetum arvense* L.) in drained areas of Lithuania: Reasons and consequences, and possibilities for its control. Acta Agriculturae Scandinavica. **56**: 25–30. 2006.

2. Hodson MJ, White PJ, Mead A, and Broadley MR. Phylogenetic variation in the silicon composition of plants. Annals of Botany. **96**: 1027–1046. 2005.

3. Myagmar BE and Aniya Y. Free radical scavenging action of medicinal herbs from Mongolia. Phytomedicine. **7**: 221–229. 2000.

4. Dos Santos JG Jr, Hoffmann MM, Marcela BM, Maria NB, Damasseno Maia F, and Kalyne AL. Cognitive enhancement in aged rats after chronic administration of *Equisetum arvense* L. with demonstrated antioxidant properties in vitro. Pharmacol Biochem Behav. **81**: 593–600. 2005.

5. Dos Santos JG Jr, Blanco MM, Do Monte FH, Russi M, Lanziotti VM, Leal LK, and Cunha GM. Sedative and anticonvulsant effects of hydroalcoholic extract of *Equisetum arvense*. Fitoterapia. **76**: 508–513. 2005.

6. Wright CI, Van-Buren L, Kroner CI, and Koning MM. Herbal medicines as diuretics: review of the scientific evidence. J Ethnopharmcol. **114**: 1–31. 2007.

7. Miwa Y and Sakuma R. A safety toxicology study of *Equisetum arvense* L. Pharmacometrics. **76**: 61–69. 2009.

8. Sudan BJ. Seborrhoeic dermatitis induced by nicotine of horsetails (*Equisetum arvense* L.). Contact Dermatitis. **13**: 201-202. 1985.

9. Doi AM, Hill G, Seely J, Hailey JR, Kissling G, and Bucher JR. Alpha 2u-globulin nephropathy and renal tumors in national toxicology program studies. Toxicol Pathol. **35**: 533–540. 2007

10. Rao GN. Diet and kidney diseases in rats. Toxicol Pathol. **30**: 651–656. 2002.

11. Maeda H, Miyamoto K, and Sano T. Occurrence of dermatitis in rats fed a cholesterol diet containing field horsetail (*Equisetum arvense* L.). J Nutr Sci Vitaminol. **43**: 553–563. 1997.

12. Glick ZR, Saedi N, and Ehrlich A. Allergic contact dermatitis from cigarettes. Dermatitis. **20**: 6–13. 2009.

Low-dose carcinogenicity of 2-amino-3-methylimidazo[4,5-f]quinoline in rats: Evidence for the existence of no-effect levels and a mechanism involving p21$^{Cip/WAF1}$

Min Wei,[1] Hideki Wanibuchi,[1] Dai Nakae,[2] Hiroyuki Tsuda,[3] Satoru Takahashi,[4] Masao Hirose,[5] Yukari Totsuka,[6] Masae Tatematsu,[7] and Shoji Fukushima[7,8]

[1]Department of Pathology, Osaka City University Medical School, Osaka; [2]Department of Environmental Health and Toxicology, Tokyo Metropolitan Institute of Public Health, Tokyo; Departments of [3]Molecular Toxicology and [4]Experimental Pathology and Tumor Biology, Nagoya City University Graduate School of Medical Sciences, Nagoya; [5]Food Safety Commission, Tokyo; [6]Cancer Prevention Basic Research Project, National Cancer Center Research Institute, Tokyo; [7]Japan Bioassay Research Center, Kanagawa, Japan

The carcinogenicity of the low amounts of genotoxic carcinogens present in food is of pressing concern. The purpose of the present study was to determine the carcinogenicity of low doses of the dietary genotoxic carcinogen 2-amino-3-methylimidazo[4,5-f]quinoline (IQ) and to investigate mechanisms by which IQ exerts its carcinogenic effects. A total of 1595 male F344 rats were divided into seven groups and administered with IQ at doses of 0, 0.001, 0.01, 0.1, 1, 10 and 100 p.p.m. in the diet for 16 weeks. We found that IQ doses of 1 p.p.m. and below did not induce preneoplastic lesions in either the liver or the colon, while IQ doses of 10 and 100 p.p.m. induced preneoplastic lesions in both of these organs. These results demonstrate the presence of no-effect levels of IQ for both liver and colon carcinogenicity in rats. The finding that p21$^{Cip/WAF1}$ was significantly induced in the liver at doses well below those required for IQ mediated carcinogenic effects suggests that induction of p21$^{Cip/WAF1}$ is one of the mechanisms responsible for the observed no-effect of low doses of IQ. Furthermore, IQ administration caused significant induction of CYP1A2 at doses of 0.01–10 p.p.m., but administration of 100 p.p.m. IQ induced CYP1A1 rather than CYP1A2. This result indicates the importance of dosage when interpreting data on the carcinogenicity and metabolic activation of IQ. Overall, our results suggest the existence of no-effect levels for the carcinogenicity of this genotoxic compound. (*Cancer Sci* 2011; 102: 88–94)

E xposure to environmental carcinogens is one of the most significant causes of human cancers. Determination of the dose-response relationship between carcinogen exposure and induction of cancer is one of the most important areas of chemical risk assessment. Of particularly high priority is the cancer risk assessment of dietary carcinogens.

Heterocyclic amines (HCA) are well known dietary genotoxic carcinogens derived from cooked protein-rich foods such as meat and fish,[1–3] and the carcinogenicities of 2-amino-3,8-dimethylimidazo[4,5-f]quinoxaline (MeIQx), 2-amino-1-methyl-6-phenylimidazo[4,5-b]pyridine (PhIP) and 2-amino-3-methylimidazo[4,5-f]quinoline (IQ) have been widely investigated in various animal models. MeIQx induces cancers of the liver, zymbal gland, skin and clitoral gland in rats,[4] and caners of the liver and lung, and lymphoma and leukemia in mice.[5] PhIP induces colon cancers and mammary gland cancers in rats,[6] and lymphomas in mice.[7] IQ induces cancers of the liver, colon, mammary and zymbal glands in rats, caners of the liver, lung and forestomach in mice, and cancer of the liver in non-human primates.[8–10] MeIQx and PhIP are classified as category

2B compounds (possibly carcinogenic to humans) and IQ is classified as a category 2A compound (probably carcinogenic to humans) by the International Agency for Research on Cancer.[11] Therefore, although the concentrations of HCA in food are low, they constitute a potential hazard, and there is concern regarding the carcinogenic effects of low doses of these HCA.

Based on the view that even minute doses of a genotoxic carcinogen has the potential to produce irreversible deleterious genetic changes in the DNA of a target organ cell and the argument that if sufficient numbers of test animals are used the carcinogenic effect of a minute dose can be demonstrated, it is generally assumed that genotoxic carcinogens exert a non-threshold carcinogenic effect. However, the carcinogenicities of most genotoxic carcinogens are determined by experimental animal carcinogenicity studies using doses that are generally orders of magnitude higher than actual human exposure levels and the dose-response curves obtained are then extrapolated to zero using a non-threshold mathematical model. This approach, however, is being challenged as advancements in the understanding of the molecular mechanisms of carcinogenesis are being made and experimental evidence showing that genotoxic carcinogens do not exert mutagenic and carcinogenic effects at low doses accumulates.[12–19]

Previously, we demonstrated the existence of no-effect levels of MeIQx for both hepatocarcinogenicity and *in vivo* mutagenicity in various carcinogenesis models in different rat strains.[17,20–22] It has also been shown that low doses of PhIP do not exert either initiation or promotion activities in colon carcinogenesis in the rat.[23,24] However, little is known about the carcinogenic potential of low doses of IQ.

In addition, little is known about the mechanisms underlying the carcinogenicities of lower doses of HCA, but incorporation of mechanistic information is critical for quantitative cancer risk assessment. The purpose of the present study is to determine the relationship between administration of low doses of IQ and induction of preneoplastic lesions in the liver and colon in rats, and to investigate carcinogenic mechanisms of action of various doses of IQ by evaluating DNA-adduct formation, oxidative DNA damage and expression levels of genes involved in metabolic activation of IQ, cell proliferation and DNA damage repair in the liver.

---

[8]To whom correspondence should be addressed.
E-mail: s-fukushima@jisha.or.jp

Materials and Methods

Chemical and diets. IQ was purchased from Nard Institute Ltd (Osaka, Japan) with a purity of 99.9%. Basal diets (powdered MF; Oriental Yeast Co., Tokyo, Japan) and the diets containing IQ were prepared once a month by Oriental Yeast Co.

Animals. A total of 1595 male F344 rats were supplied by Charles River Japan, Inc. (Hino, Shiga, Japan) and were used at 21 days of age. Animals were housed in polycarbonate cages (five per cage) in experimental animal rooms with a targeted temperature of $22 \pm 3°C$, relative humidity of $55 \pm 5\%$ and a 12-h light/dark cycle. Diet and tap water were available *ad libitum* throughout the study.

Experimental design. The animal experiment protocols were approved by the Institutional Animal Care and Use Committee of Osaka City University Medical School. Rats were randomized into seven groups, 245 rats in each of groups 1–6 and 125 rats in group 7. Since the levels of IQ in cooked foods are lower than those of MeIQx and PhIP,[11] IQ dosage and treatment duration in this study were the same as the previous low dose carcinogenicity studies with MeIQx and PhIP.[18,24] Animals were fed diets containing IQ as follows: 0 (group 1, control), 0.001 (group 2), 0.01 (group 3), 0.1 (group 4), 1 (group 5), 10 (group 6) and 100 p.p.m. (group 7) for 16 weeks. Fresh diet was supplied to the animals twice weekly. Bodyweights, food consumption and water intake were measured weekly.

Five rats in each group were killed at week 4 under ether anesthesia. At death, livers were snap frozen in liquid nitrogen and stored at −80°C for examination of IQ-DNA adducts and 8-hydroxy-2′-deoxyguanosine (8-OHdG) formation in the DNA. The remaining rats were killed at the end of week 16 under ether anesthesia for examination of the development of glutathione S-transferase placental form (GST-P) positive foci, which is a well-established preneoplastic lesion in the rat liver,[25,26] and aberrant crypt foci (ACF), which is a surrogate marker for preneoplastic lesions in the rat colon.[24,27,28] At death, livers were excised, weighed and then three slices each from the left lateral, medial and right lateral lobes were cut and placed in 10% phosphate-buffered formalin. The remaining liver tissues were snap frozen in liquid nitrogen and stored at −80°C for mRNA expression analysis. Following fixation, liver tissues were embedded in paraffin and processed for histopathological examination.

Examination of GST-P positive foci in the liver. Anti-rat GST-P polyclonal antibody (Medical and Biological Laboratories Co., Ltd, Nagoya, Japan) at a dilution of 1:1000 was used for immunohistochemical staining of GST-P. The GST-P-positive hepatocellular foci composed of two or more cells were counted under a light microscope.[17,18,20,22] Total areas of livers were measured using a color image processor IPAP (Sumica Technos, Osaka, Japan) and the number of GST-P-positive foci per square centimeter of liver tissue was calculated.

IQ-DNA adduct and 8-OHdG formation in livers. IQ-DNA adducts were measured by the ^{32}P-postlabeling method as described previously.[29,30] Levels of 8-OHdG formation in liver DNA were determined by high-performance liquid chromatography with electrochemical detection as previously described.[31]

TaqMan real-time quantitative PCR. The mRNA expression levels of genes involved in IQ metabolism (CYP1A1, CYP1A2 and CYP1B1), DNA damage repair (8-oxoguanine DNA glycosylase [Ogg1], growth arrest and DNA damage-inducible protein 45 [GADD45], AP endonuclease-1 [APE-1], MSH2 and MSH3) and cell cycle regulation (p53 and $p21^{Cip/WAF1}$ and proliferating cell nuclear antigen [PCNA]) were evaluated in the livers by TaqMan real-time quantitative PCR as described previously.[31] Sequence-specific primers and probes (Taqman Gene Expression Assay) were purchased from Applied Biosystems, Inc., Carlsbad, CA, USA. Beta-2-microglobulin (B2M) was used as an internal control.

Examination of ACF in colon. Formation of ACF was examined as described previously.[24] Although ACF consisting of four or more crypts are considered to be better predictors of colon tumor outcome in rats,[32] to ensure that all doses of IQ that have the potential to induce colon carcinogenesis were accounted for, doses of IQ that caused an increase of any size of ACF were considered to have the potential to induce colon carcinogenesis in the present study.[24]

Statistical analysis. All mean values are reported as mean ± SD. Statistical analyses were performed using the Statlight program (Yukms Co., Ltd, Tokyo, Japan). Homogeneity of variance was tested by the Bartlett test. Differences in mean values between the control and IQ-treated groups were evaluated by the 2-tailed Dunnett test when variance was homogeneous and the 2-tailed Steel test when variance was heterogeneous.[22,31] P values <0.05 were considered significant.

Results

General observation. All animals survived to the end of study without any apparent abnormal pathological features. The final average body and liver weights and IQ intake are summarized in Table 1. The final bodyweight of the 100 p.p.m. group was significantly lower than that of the 0 p.p.m. group. Absolute and relative liver weights were significantly decreased in the 0.1 and 1 p.p.m. groups and were significantly increased in the 100 p.p.m. group compared with the 0 p.p.m. group. There were no significant differences in either food or water consumption among groups (data not shown). The intake of IQ was proportional to the administered doses (Table 1). No tumors were found in any organs including the liver and colon in any of the groups.

Induction of GST-P-positive foci in the livers. No histopathological changes were observed in any of the IQ-treated groups.

Table 1. Body and organ weights, and IQ intake

| Group | IQ (p.p.m.) | No. rats | Bodyweight (g) | Liver | | Average IQ intake | |
				Absolute weight (g)	Relative weight (%)	Daily intake (mg/kg b.w.)	Total (mg/kg b.w.)
1	0	240	331 ± 23	9.3 ± 1.7	2.8 ± 0.4	0	
2	0.001	240	332 ± 17	9.1 ± 1.4	2.8 ± 0.4	0.0001	0.008
3	0.01	240	331 ± 19	9.0 ± 1.5	2.8 ± 0.4	0.0007	0.08
4	0.1	240	331 ± 22	8.5 ± 1.2*	2.6 ± 0.3*	0.008	0.9
5	1	240	331 ± 17	8.5 ± 1.2*	2.6 ± 0.3*	0.08	8.7
6	10	240	330 ± 18	9.0 ± 1.3	2.7 ± 0.4	0.76	85.1
7	100	120	319 ± 19*	10.0 ± 1.6*	3.2 ± 0.4*	7.83	877.5

*Significantly different from group 1. IQ, 2-amino-3-methylimidazo[4,5-*f*]quinoline.

The number and size of GST-P-positive foci in rat livers at week 16 is summarized in Table 2. The total numbers of GST-P-positive foci per unit area in the livers in the groups administered 0.001–1 p.p.m. IQ did not differ from the control value (0 p.p.m. group), and no significant increases were observed in any size range of GST-P-positive foci in these groups. Significant increases in the total numbers of GST-P-positive foci per unit area in the liver were observed in the 10 and 100 p.p.m. groups compared with the control. The numbers of GST-P-positive foci composed of 2–4 cells and 5–10 cells in the 10 p.p.m. group and GST-P-positive foci of all sizes in the 100 p.p.m. group were significantly increased.

Formation of IQ-DNA adduct and 8-OHdG in liver DNA. Representative autoradiograms of IQ-DNA adducts in livers are shown in Figure 1. The levels of IQ-DNA adducts in the livers of the 0 and 0.001 p.p.m. IQ-treated groups were under the detectable limit at week 4 (Table 3). IQ-DNA adducts were detectable in the livers of rats administered 0.01 p.p.m. IQ, and adduct formation increased in a dose-dependent manner in groups administered higher doses of IQ. No significant differences in 8-OHdG levels were observed in the liver DNA between any of the groups administered IQ and the control group (Table 3).

Gene expression changes in the liver. Relative mRNA expression of IQ metabolizing genes CYP1A 1and CYP1A2, cell cycle genes PCNA and p21$^{Cip/WAF1}$, p53, and DNA repair genes APE-1 and GADD45 in the livers at week 16 is shown in Figure 2. CYP1A1 was significantly increased in the livers of rats treated with 100 p.p.m. IQ, but not in the lower doses of IQ. CYP1A2, on the other hand, was significantly increased in the 0.01–10 p.p.m. groups, but no significant change was observed in the 100 p.p.m. group. There was no significant difference in the CYP1B1 expression level among groups (data not shown).

A significant increase in PCNA was observed in the 100 p.p.m. group, but not in the groups administered lower doses of IQ, while the negative cell cycle regulator p21$^{Cip/WAF1}$ was significantly induced in the 0.01 p.p.m. group and maximally induced in the 100 p.p.m. group. The expression level of p21$^{Cip/WAF1}$ in the 100 p.p.m. group was significantly higher than in the 10 p.p.m. and lower dose groups. There were no significant changes in p53 expression levels in the IQ-treated groups.

APE-1 was significantly induced in the 10 and 100 p.p.m. groups and GADD45 was significantly induced in the 100 p.p.m. group. IQ had no effect on the expression of Ogg-1, MSH2 or MSH3 (data not shown).

Induction of ACF in the colon. The number and size of ACF in rat colons at week 16 is summarized in Table 4. In the 10 p.p.m. group, the number of ACF composed of one crypt was significantly increased compared with the control. In the 100 p.p.m. group, significant increases were observed in the numbers of all sizes of ACF. In contrast, in the groups administered 0.001–1 p.p.m. IQ, neither the number of any size ACF nor the total number of ACF differed from the control.

Discussion

Dose-response relationships for genotoxic carcinogens have been a topic of intense scientific and public debate. High doses of the genotoxic dietary carcinogen IQ have been demonstrated to induce liver and colon cancers in rats (300 p.p.m. in diet)[8] and liver cancers in nonhuman primates (10 mg/kg b.w./day).[10] However, as the concentrations of IQ in food are generally extremely low,[11] there is uncertainty regarding the carcinogenicity of the doses of IQ to which humans are exposed. The present study shows that IQ at doses of 1 p.p.m. (0.08 mg/kg body weight [b.w.]/day) and lower did not induce either GST-P-positive foci in the liver or ACF in the colon. Only in the groups administered higher doses of IQ, 10 p.p.m. (0.76 mg/kg b.w./day) and 100 p.p.m. (7.83 mg/kg b.w./day), were increases in GST-P-positive foci and ACF observed.

GST-P-positive foci and ACF are well-established preneoplastic lesions of the liver and colon, respectively, in rats. These lesions have been accepted as useful end-point markers in the assessment of carcinogenic effects of environmentally relevant concentrations of carcinogens as they can extend the range of observable effect levels.[24,26] Therefore, the results of the present study suggest the presence of no-effect levels of IQ for both liver and colon carcinogenicity in rats and indicate that the dose-response relationship for carcinogenicity of low dose IQ is nonlinear.

Several threshold mechanisms for genotoxic carcinogens have been suggested, including induction of detoxification processes, cell cycle delay, DNA repair, apoptosis and the suppression of neoplastically transformed cells by the immune system.[12,13,15,33] However, little in vivo evidence is available. To explore mechanisms underlying the carcinogenicity of low doses of IQ, we examined the relative mRNA expression of a panel of genes involved in cell proliferation, cell cycle regulation, DNA repair and IQ metabolic activation. We found that the cell proliferation marker PCNA was significantly increased only at a dose of 100 p.p.m., a dose that is carcinogenic. The cell cycle negative regulator p21$^{Cip/WAF1}$, on the other hand, was significantly induced at a dose of 0.01 p.p.m., a dose well below that which induced the formation of preneoplastic lesions. Furthermore, the finding that the levels of p21$^{Cip/WAF1}$ in the groups administered 10 p.p.m. and less were much lower than that of the group administered 100 p.p.m. implies that hepatocytes have adequate capacity to cope with the type of damage that is repaired by the p21$^{Cip/WAF1}$ pathway when exposed to low doses of IQ, but that the repair capacity of these hepatocytes, even in the presence of high p21$^{Cip/WAF1}$ expression, can be overwhelmed when the cell is subjected to very high doses of IQ. It is reasonable to suggest

Table 2. Development of GST-P-positive foci in the livers of rats administered IQ for 16 weeks

Group	IQ (p.p.m.)	No. rats	Size of GST-P positive foci				
			2–4	5–10	11–20	≥21	Total
1	0	240	0.09 ± 0.25	0.03 ± 0.11	0.02 ± 0.11	0.00 ± 0.02	0.15 ± 0.31
2	0.001	240	0.10 ± 0.24	0.04 ± 0.15	0.01 ± 0.07	0	0.16 ± 0.31
3	0.01	240	0.15 ± 0.47	0.07 ± 0.41	0.02 ± 0.22	0.02 ± 0.03	0.26 ± 1.30
4	0.1	240	0.10 ± 0.28	0.04 ± 0.15	0.01 ± 0.07	0.01 ± 0.08	0.15 ± 0.35
5	1	240	0.10 ± 0.25	0.04 ± 0.16	0.01 ± 0.06	0	0.14 ± 0.33
6	10	240	0.51 ± 0.65	0.19 ± 0.36*	0.02 ± 0.10	0.01 ± 0.11	0.74 ± 0.88*
7	100	120	26.23 ± 18.24*	23.81 ± 16.23*	19.25 ± 11.70*	18.74 ± 11.81*	88.03 ± 50.41*

*Significantly different from group 1. GST-P, glutathione S-transferase placental form positive foci; IQ, 2-amino-3-methylimidazo[4,5-f]quinoline.

Fig. 1. Autoradiograms of 2-amino-3-methylimidazo-[4,5-*f*]quinoline (IQ)-DNA adducts the livers of 0 (a), 0.001 (b) and 100 (c) p.p.m. IQ-treated groups at week 4. Arrowheads indicate IQ-DNA adduct. The imaging plates were exposed for 3 h (a) and 24 h (b and c).
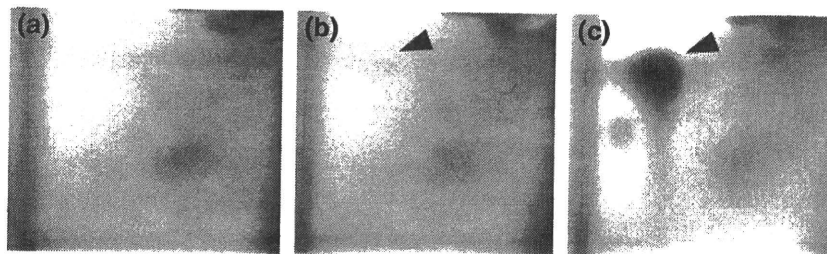
Table 3. IQ-DNA adduct and 8-OHdG formation in liver DNA

Group	IQ (p.p.m.)	No. rats	Adduct level ($\times 10^{-7}$ ntd)	8-OHdG ($\times 10^{-5}$ dG)
1	0	5	UDL	0.23 ± 0.07
2	0.001	5	UDL	0.25 ± 0.05
3	0.01	5	0.045 ± 0.02	0.24 ± 0.07
4	0.1	5	0.1 ± 0.004	0.32 ± 0.10
5	1	5	1.7 ± 0.07	0.24 ± 0.08
6	10	5	12.7 ± 0.07	0.22 ± 0.07
7	100	5	107.0 ± 0.07	0.23 ± 0.08

IQ, 2-amino-3-methylimidazo[4,5-*f*]quinoline; ntd, nucleotide; 8-OHdG: 8-hydroxy-2′-deoxyguanosine; UDL, under the detectable limit.

that suppression of cell cycle progression by p21$^{Cip/WAF1}$ followed by DNA repair is at least one of the mechanisms responsible for the observed no-effect of low doses of IQ in rats in the present model.

It is known that the vast majority of DNA damage is repaired by base excision repair (BER), nucleotide excision repair (NER) and mismatch repair (MMR).[34] APE-1 plays an essential role in the BER repair process by cleaving the phosphodiester backbone.[35] The activities of two different heterodimeric complexes, MSH2-MSH3 and MSH2-MSH6, belonging to the MMR system are mainly responsible for the post-replicative repair of mismatches.[36] We found that IQ significantly increased the expression levels of APE-1 but not MSH2 and MSH3 at doses of 10 and 100 p.p.m. in the liver. It has also been reported that IQ has no effect on expression of ERCC1, which is a key molecule in the NER process.[37] These findings suggest that BER rather than MMR or NER responds to IQ-induced DNA damage.

GADD45 is involved in a variety of growth regulatory mechanisms, including DNA repair, growth arrest and apoptosis.[38] It is induced by genotoxic and certain other cell stresses by p53-dependent and independent pathways.[39,40] GADD45 expression was significantly induced in the 100 p.p.m. group. The fact that significant induction of APE-1 and GADD45 was observed only at the highest doses of 10 and/or 100 p.p.m. indicate the IQ-induced DNA damage response is dose-dependent. Moreover, the fact that in the groups with low doses expression of APE-1 and GADD45 were not affected and that there was a significant but moderate induction of p21$^{Cip/WAF1}$ imply that normal physiological levels of these genes are sufficient to repair the DNA damage caused by low doses of IQ. However, the expression levels of these genes are all increased by higher carcinogenic doses of IQ. A reasonable explanation of the no-effect of low doses of IQ and the carcinogenicity of high doses of IQ is that carcinogenicity is the consequence of a disruption in the balance between DNA damage and repair and between abnormal cell proliferation and apoptosis or cell cycle regulation.

Our results show that p53 gene expression is not induced by administration of IQ. Furthermore, p53-deficient mice do not show higher susceptibility to IQ-induced liver carcinogenesis than wild type mice.[41] These results suggest that p53 does not have a significant impact on the carcinogenicity of IQ.

DNA adduct formation by metabolic activation of IQ is believed to play an important role in the carcinogenicity of IQ.[42] Formation of IQ-DNA adducts in the liver showed a linear dose-dependency and proved to be one of the most sensitive end-points for the detection of exposure to IQ. Adduct formation was detectable in groups administered far lower doses of IQ compared with detection of other end-points such as cell proliferation and preneoplastic lesion induction. That IQ-DNA adduct formation was not detected in the 0.001 p.p.m. group was most likely due to the detection limit of the assay. It should be noted that DNA adduct is a premutagenic lesion and not necessarily correlated to the frequencies of mutation and cancer induced by genotoxic compounds. For example, it is known that IQ forms DNA adducts in the kidneys and stomach of both rats and monkeys, but does not induce tumors in these organs.[43,44] Our present findings of a linear dose-response of IQ-DNA adduct formation and a nonlinear carcinogenic dose-response to IQ administration support the idea that IQ-DNA adducts do not necessarily lead to mutation and formation of cancerous lesions. Our results are also in line with previous results on HCA including MeIQx[1,18,45] and PhIP.[24] These results can be explained, at least in part, by the actions of gene products such as p21$^{Cip/WAF1}$, GADD45 and APE-1 and the other repair genes for DNA damage. Moreover, in the case of MeIQx, it has been suggested that formation of DNA adducts alone might not be sufficient to produce cancers and that the MeIQx-induced genetic alterations in the liver are enhanced by liver regeneration induced by high doses of MeIQx itself.[1] Therefore, while IQ-DNA adduct formation is important in IQ carcinogenicity, high levels of adduct formation are likely required and other factors such as cell proliferation can affect the balance between DNA damage and repair and lead to fixation of DNA mutations into the cell's genome.

It has been demonstrated *in vitro* that IQ is more efficiently metabolized and activated by CYP1A2 than by CYP1A1 or CYP1B1.[46] However, limited *in vivo* data are available. In a study by McPherson *et al.*[47], no significant induction in mRNA expression level or activity of either CYP1A1 or CYP1A2 were reported in the livers of rats receiving 300 p.p.m. IQ in the diet for 52 weeks, but these enzymes were significantly increased after daily administration of 20 mg/kg b.w. IQ by oral gavage for 3 days; in the average adult rat, a dose of 300 p.p.m. IQ in the diet is approximately equivalent to administration of 20 mg/kg b.w. IQ by oral gavage. The results of the present study revealed that IQ significantly induced CYP1A2 expression at doses from 0.01 to 10 p.p.m., but CYP1A2 was not induced in the 100 p.p.m. group. The lack of effect of 100 p.p.m. IQ on CYP1A2 expression is consistent with the results in rats receiving 300 p.p.m. IQ in the diet for 52 weeks.[47] Significant increases in CYP1A1 expression in the 100 p.p.m. group provide an alternative mechanism that can compensate for decreased CYP1A2 activity. However, as noted above, in apparent contrast to our results, in the study by McPherson *et al.*,[47] administration of 300 p.p.m. IQ over the course of 52 weeks did
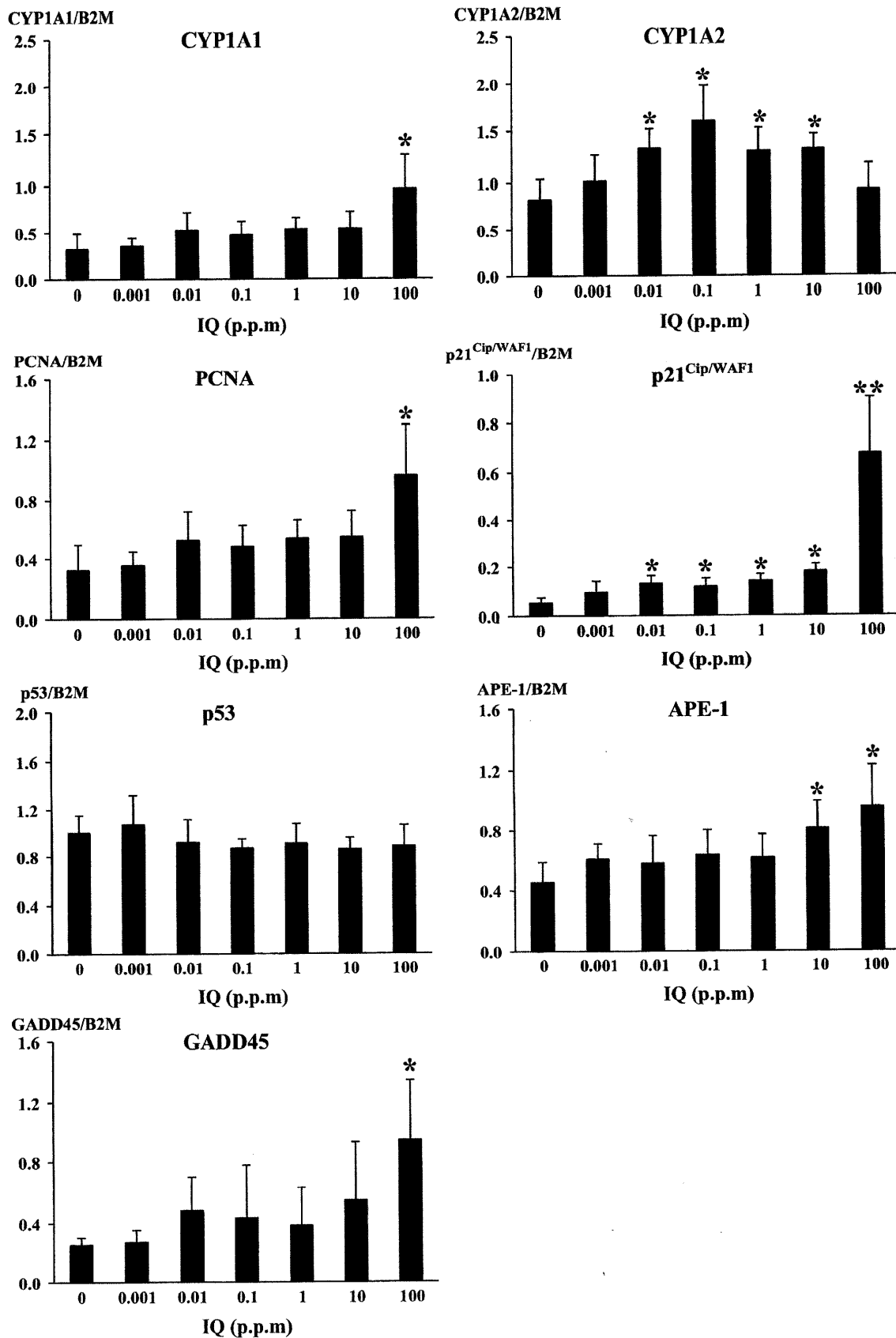
CYP1A1/B2M

CYP1A1

2.5
2.0
1.5
1.0
0.5
0.0

*

0   0.001   0.01   0.1   1   10   100

IQ (p.p.m)

CYP1A2/B2M

CYP1A2

2.5
2.0
1.5
1.0
0.5
0.0

*   *   *   *

0   0.001   0.01   0.1   1   10   100

IQ (p.p.m)

PCNA/B2M

PCNA

1.6
1.2
0.8
0.4
0.0

*

0   0.001   0.01   0.1   1   10   100

IQ (p.p.m)

p21$^{Cip/WAF1}$/B2M

p21$^{Cip/WAF1}$

1.0
0.8
0.6
0.4
0.2
0.0

**

*   *   *   *

0   0.001   0.01   0.1   1   10   100

IQ (p.p.m)

p53/B2M

p53

2.0
1.6
1.2
0.8
0.4
0.0

0   0.001   0.01   0.1   1   10   100

IQ (p.p.m)

APE-1/B2M

APE-1

1.6
1.2
0.8
0.4
0.0

*   *

0   0.001   0.01   0.1   1   10   100

IQ (p.p.m)

GADD45/B2M

GADD45

1.6
1.2
0.8
0.4
0.0

*

0   0.001   0.01   0.1   1   10   100

IQ (p.p.m)

Fig. 2. Relative mRNA expression in the livers of rats at week 16. *Significantly different from 0 p.p.m. **Significantly different from all other groups. APE-1, AP endonuclease-1; B2M, beta-2-microglobulin; GADD45, growth arrest and DNA damage-inducible protein 45; PCNA, proliferating cell nuclear antigen.

Table 4. Development of ACF in the colons of rats administered IQ for 16 weeks

Group	IQ (p.p.m.)	No. rats	Size of ACF				
			1	2	3	≥4	Total
1	0	240	0.08 ± 0.28	0.12 ± 0.32	0.06 ± 0.25	0.08 ± 0.29	0.33 ± 0.64
2	0.001	240	0.12 ± 0.36	0.08 ± 0.29	0.10 ± 0.32	0.09 ± 0.30	0.39 ± 0.69
3	0.01	240	0.15 ± 0.41	0.15 ± 0.42	0.06 ± 0.24	0.06 ± 0.24	0.43 ± 0.77
4	0.1	240	0.11 ± 0.33	0.11 ± 0.35	0.06 ± 0.25	0.08 ± 0.27	0.36 ± 0.63
5	1	240	0.15 ± 0.45	0.10 ± 0.30	0.10 ± 0.33	0.05 ± 0.23	0.41 ± 0.80
6	10	240	0.19 ± 0.48*	0.16 ± 0.41	0.07 ± 0.25	0.09 ± 0.40	0.50 ± 0.86
7	100	120	1.48 ± 1.46*	1.29 ± 1.51*	0.70 ± 0.93*	0.72 ± 1.01*	4.19 ± 3.34*

*Significantly different from group 1. ACF, aberrant crypt foci; IQ, 2-amino-3-methylimidazo[4,5-f]quinoline.

not induce CYP1A1. Therefore, it is reasonable to postulate that the dose-relationship between IQ and induction of CYP1A1 is not a simple dose-response. CYP1B1 does not appear to be involved in the metabolism of IQ at doses up to 100 p.p.m. in rats. The findings described above demonstrate the importance of taking into account dosage, duration and route of exposure in interpretation of the data on metabolic activation of IQ. Further studies on the dose-response relationships between chronic IQ exposure and the protein expression levels and activities of detoxifying enzymes, especially at doses relevant to human exposure, would provide further insight into the role of metabolic activation in IQ carcinogenicity.

Oxidative DNA damage does not appear to play a role in IQ-induced carcinogenesis. In the present study, no significant changes in 8-OHdG levels or Ogg1 expression levels in the livers of IQ-treated rats were observed. Our results are consistent with the recent findings in IQ-treated Big Blue rats that oxidative stress was not responsible for the initiation of IQ-induced carcinogenesis in the liver and colon.[37] In this respect, IQ is different from MeIQx, in which oxidative DNA damage plays an important role in liver carcinogenesis.[48]

In summary, the present study provides the first experimental data on the carcinogenicity of low doses of IQ in both the liver and colon of the test animal and compares the effect of IQ at the cellular level with its carcinogenic effect. Our findings support the idea that there is a practical threshold that should be considered when evaluating the risk of genotoxic carcinogens. To this end, further accumulation of data, especially mechanistic data, should be promoted to facilitate not only an understanding of the carcinogenic effects of low doses of genotoxic carcinogens but also to establish an accurate means of quantitative risk assessment.

Acknowledgments

Disclosure Statement

The authors have no conflict of interest.

References

1 Wakabayashi K, Nagao M, Esumi H, Sugimura T. Food-derived mutagens and carcinogens. *Cancer Res* 1992; **52**: 2092s–8s.
2 Layton DW, Bogen KT, Knize MG, Hatch FT, Johnson VM, Felton JS. Cancer risk of heterocyclic amines in cooked foods: an analysis and implications for research. *Carcinogenesis* 1995; **16**: 39–52.
3 Nagao M, Ushijima T, Toyota M, Inoue R, Sugimura T. Genetic changes induced by heterocyclic amines. *Mutat Res* 1997; **376**: 161–7.
4 Kato T, Ohgaki H, Hasegawa H, Sato S, Takayama S, Sugimura T. Carcinogenicity in rats of a mutagenic compound, 2-amino-3,8-dimethylimidazo[4,5-f]quinoxaline. *Carcinogenesis* 1988; **9**: 71–3.
5 Ohgaki H, Hasegawa H, Suenaga M, Sato S, Takayama S, Sugimura T. Carcinogenicity in mice of a mutagenic compound, 2-amino-3,8-dimethylimidazo[4,5-f]quinoxaline (MeIQx) from cooked foods. *Carcinogenesis* 1987; **8**: 665–8.
6 Ito N, Hasegawa R, Sano M et al. A new colon and mammary carcinogen in cooked food, 2-amino-1-methyl-6-phenylimidazo[4,5-b]pyridine (PhIP). *Carcinogenesis* 1991; **12**: 1503–6.
7 Esumi H, Ohgaki H, Kohzen E, Takayama S, Sugimura T. Induction of lymphoma in CDF1 mice by the food mutagen, 2-amino-1-methyl-6-phenylimidazo[4,5-b]pyridine. *Jpn J Cancer Res* 1989; **80**: 1176–8.
8 Ohgaki H, Hasegawa H, Kato T et al. Carcinogenicity in mice and rats of heterocyclic amines in cooked foods. *Environ Health Perspect* 1986; **67**: 129–34.
9 Ohgaki H, Kusama K, Matsukura N et al. Carcinogenicity in mice of a mutagenic compound, 2-amino-3-methylimidazo[4,5-f]quinoline, from broiled sardine, cooked beef and beef extract. *Carcinogenesis* 1984; **5**: 921–4.
10 Adamson RH, Thorgeirsson UP, Snyderwine EG et al. Carcinogenicity of 2-amino-3-methylimidazo[4,5-f]quinoline in nonhuman primates: induction of tumors in three macaques. *Jpn J Cancer Res* 1990; **81**: 10–4.
11 WHO, IARC. *IARC Monographs on the Evaluation of Carcinogenic Risks to Humans: Some Naturally Occurring Substances: Food Items and Constituents, Heterocylic Aromatic Amines and Mycotoxins.* Lyon: World Health Organization, International Agency for Research on Cancer, 1993; 165–242.
12 Sofuni T, Hayashi M, Nohmi T, Matsuoka A, Yamada M, Kamata E. Semi-quantitative evaluation of genotoxic activity of chemical substances and evidence for a biological threshold of genotoxic activity. *Mutat Res* 2000; **464**: 97–104.
13 De Flora S. Detoxification of genotoxic compounds as a threshold mechanism limiting their carcinogenicity. *Toxicol Pathol* 1984; **12**: 337–43.
14 Kirkland DJ, Muller L. Interpretation of the biological relevance of genotoxicity test results: the importance of thresholds. *Mutat Res* 2000; **464**: 137–47.
15 Lutz WK, Kopp-Schneider A. Threshold dose response for tumor induction by genotoxic carcinogens modeled via cell-cycle delay. *Toxicol Sci* 1999; **49**: 110–5.
16 Parry JM. Reflections on the implications of thresholds of mutagenic activity for the labelling of chemicals by the European Union. *Mutat Res* 2000; **464**: 155–8.
17 Hoshi M, Morimura K, Wanibuchi H et al. No-observed effect levels for carcinogenicity and for in vivo mutagenicity of a genotoxic carcinogen. *Toxicol Sci* 2004; **81**: 273–9.
18 Fukushima S, Wanibuchi H, Morimura K et al. Lack of a dose-response relationship for carcinogenicity in the rat liver with low doses of 2-amino-3,8-dimethylimidazo[4,5-f]quinoxaline or N-nitrosodiethylamine. *Jpn J Cancer Res* 2002; **93**: 1076–82.

19 Bolt HM, Degen GH. Human carcinogenic risk evaluation, part II: contributions of the EUROTOX specialty section for carcinogenesis. *Toxicol Sci* 2004; **81**: 3–6.

20 Fukushima S, Wanibuchi H, Morimura K *et al.* Lack of initiation activity in rat liver of low doses of 2-amino-3,8-dimethylimidazo[4,5-f]quinoxaline. *Cancer Lett* 2003; **191**: 35–40.

21 Kushida M, Wanibuchi H, Morimura K *et al.* Dose-dependence of promotion of 2-amino-3,8-dimethylimidazo[4,5-f]quinoxaline-induced rat hepatocarcinogenesis by ethanol: evidence for a threshold. *Cancer Sci* 2005; **96**: 747–57.

22 Wei M, Hori TA, Ichihara T *et al.* Existence of no-observed effect levels for 2-amino-3,8-dimethylimidazo[4,5-f]quinoxaline on hepatic preneoplastic lesion development in BN rats. *Cancer Lett* 2006; **231**: 304–8.

23 Doi K, Wanibuchi H, Salim EI *et al.* Lack of large intestinal carcinogenicity of 2-amino-1-methyl-6-phenylimidazo[4,5-b]pyridine at low doses in rats initiated with azoxymethane. *Int J Cancer* 2005; **115**: 870–8.

24 Fukushima S, Wanibuchi H, Morimura K *et al.* Existence of a threshold for induction of aberrant crypt foci in the rat colon with low doses of 2-amino-1-methyl-6-phenolimidazo[4,5-b]pyridine. *Toxicol Sci* 2004; **80**: 109–14.

25 Ito N, Tsuda H, Tatematsu M *et al.* Enhancing effect of various hepatocarcinogens on induction of preneoplastic glutathione S-transferase placental form positive foci in rats – an approach for a new medium-term bioassay system. *Carcinogenesis* 1988; **9**: 387–94.

26 Tsuda H, Fukushima S, Wanibuchi H *et al.* Value of GST-P positive preneoplastic hepatic foci in dose-response studies of hepatocarcinogenesis: evidence for practical thresholds with both genotoxic and nongenotoxic carcinogens. A review of recent work. *Toxicol Pathol* 2003; **31**: 80–6.

27 Bird RP. Observation and quantification of aberrant crypts in the murine colon treated with a colon carcinogen: preliminary findings. *Cancer Lett* 1987; **37**: 147–51.

28 Tudek B, Bird RP, Bruce WR. Foci of aberrant crypts in the colons of mice and rats exposed to carcinogens associated with foods. *Cancer Res* 1989; **49**: 1236–40.

29 Ochiai M, Nakagama H, Turesky RJ, Sugimura T, Nagao M. A new modification of the 32P-post-labeling method to recover IQ-DNA adducts as mononucleotides. *Mutagenesis* 1999; **14**: 239–42.

30 Totsuka Y, Fukutome K, Takahashi M *et al.* Presence of N2-(deoxyguanosin-8-yl)-2-amino-3,8-dimethylimidazo[4,5-f]quinoxaline (dG-C8-MeIQx) in human tissues. *Carcinogenesis* 1996; **17**: 1029–34.

31 Wei M, Hamoud AS, Yamaguchi T *et al.* Potassium bromate enhances N-ethyl-N-hydroxyethylnitrosamine-induced kidney carcinogenesis only at high doses in Wistar rats: indication of the existence of an enhancement threshold. *Toxicol Pathol* 2009; **37**: 983–91.

32 Pretlow TP, O'Riordan MA, Somich GA, Amini SB, Pretlow TG. Aberrant crypts correlate with tumor incidence in F344 rats treated with azoxymethane and phytate. *Carcinogenesis* 1992; **13**: 1509–12.

33 Kirsch-Volders M, Vanhauwaert A, Eichenlaub-Ritter U, Decordier I. Indirect mechanisms of genotoxicity. *Toxicol Lett* 2003; **140–141**: 63–74.

34 Norbury CJ, Hickson ID. Cellular responses to DNA damage. *Annu Rev Pharmacol Toxicol* 2001; **41**: 367–401.

35 Bennett RA, Wilson DM III, Wong D, Demple B. Interaction of human apurinic endonuclease and DNA polymerase beta in the base excision repair pathway. *Proc Natl Acad Sci U S A* 1997; **94**: 7166–9.

36 Kolodner RD. Guarding against mutation. *Nature* 2000; **407**: 687–9.

37 Moller P, Wallin H, Vogel U *et al.* Mutagenicity of 2-amino-3-methylimidazo[4,5-f]quinoline in colon and liver of Big Blue rats: role of DNA adducts, strand breaks, DNA repair and oxidative stress. *Carcinogenesis* 2002; **23**: 1379–85.

38 Yang Q, Manicone A, Coursen JD *et al.* Identification of a functional domain in a GADD45-mediated G2/M checkpoint. *J Biol Chem* 2000; **275**: 36892–8.

39 O'Reilly MA, Staversky RJ, Watkins RH, Maniscalco WM, Keng PC. p53-independent induction of GADD45 and GADD153 in mouse lungs exposed to hyperoxia. *Am J Physiol Lung Cell Mol Physiol* 2000; **278**: L552–9.

40 Shaulian E, Karin M. Stress-induced JNK activation is independent of Gadd45 induction. *J Biol Chem* 1999; **274**: 29595–8.

41 Morimura K, Salim EI, Yamamoto S, Wanibuchi H, Fukushima S. Dose-dependent induction of aberrant crypt foci in the livers of heterozygous p53-deficient mice treated with low dose 2-amino-3-methylimidazo [4,5-f]quinoline. *Cancer Lett* 1999; **138**: 81–5.

42 Schut HA, Snyderwine EG. DNA adducts of heterocyclic amine food mutagens: implications for mutagenesis and carcinogenesis. *Carcinogenesis* 1999; **20**: 353–68.

43 Schut HA, Herzog CR, Cummings DA. Accumulation of DNA adducts of 2-amino-3-methylimidazo[4,5-f] quinoline (IQ) in tissues and white blood cells of the Fischer-344 rat after multiple oral dosing. *Carcinogenesis* 1994; **15**: 1467–70.

44 Snyderwine EG, Yamashita K, Adamson RH *et al.* Use of the 32P-postlabeling method to detect DNA adducts of 2-amino-3-methylimidazolo[4,5-f]quinoline (IQ) in monkeys fed IQ: identification of the N-(deoxyguanosin-8-yl)-IQ adduct. *Carcinogenesis* 1988; **9**: 1739–43.

45 Yamashita K, Adachi M, Kato S *et al.* DNA adducts formed by 2-amino-3,8-dimethylimidazo[4,5-f]quinoxaline in rat liver: dose-response on chronic administration. *Jpn J Cancer Res* 1990; **81**: 470–6.

46 Shimada T, Hayes CL, Yamazaki H *et al.* Activation of chemically diverse procarcinogens by human cytochrome P-450 1B1. *Cancer Res* 1996; **56**: 2979–84.

47 McPherson RA, Tingle MD, Ferguson LR. Contrasting effects of acute and chronic dietary exposure to 2-amino-3-methyl-imidazo[4,5-f]quinoline (IQ) on xenobiotic metabolising enzymes in the male Fischer 344 rat: implications for chemoprevention studies. *Eur J Nutr* 2001; **40**: 39–47.

48 Kato T, Hasegawa R, Nakae D *et al.* Dose-dependent induction of 8-hydroxyguanine and preneoplastic foci in rat liver by a food-derived carcinogen, 2-amino-3,8-dimethylimidazo[4,5-f]quinoxaline, at low dose levels. *Jpn J Cancer Res* 1996; **87**: 127–33.

Mitochondrial Prohibitins and Septin 9 Are Implicated in the Onset of Rat Hepatocarcinogenesis

Anna Kakehashi,* Naomi Ishii,* Takeshi Shibata,† Min Wei,* Etsuko Okazaki,‡ Taro Tachibana,‡ Shoji Fukushima,*[,1] and Hideki Wanibuchi*[,2]

*Department of Pathology, Osaka City University Medical School, Abeno-ku, Osaka 545-8585, Japan; †K.K. AB Sciex, Chuo-ku, Tokyo 104-0032, Japan; and ‡Department of Bioengineering, Graduate School of Engineering, Osaka City University, Sumiyoshi-ku, Osaka 558-8585, Japan

[1]Present address: Japan Bioassay Research Center, 2445 Hirasawa, Hadano, Kanagawa 257-0015, Japan.
[2]To whom correspondence should be addressed at the Department of Pathology, Osaka City University Medical School, Asahi-machi 1-4-3, Abeno-ku, Osaka 545-8585, Japan. Fax: 81-6-6646-3093. E-mail: wani@med.osaka-cu.ac.jp.

In the present study, protein lysates from microdissected glutathione S-transferase placental-form–positive (GST-P+) foci and hepatocellular carcinomas from livers of rats treated with N-diethylnitrosamine followed by phenobarbital at doses of 0 and 500 ppm in the diet for 10 and 33 weeks were analyzed using QSTAR Elite liquid chromatography with tandem mass spectrometry and iTRAQ technology. Among 75 proteins, a total of 27 and 50 proteins displaying significant quantitative changes comparing with adjacent normal-appearing liver tissue were identified in GST-P+ foci of initiation control and promotion groups, respectively, which are related to transcription, protein folding, cytoskeleton filaments reorganization, cell cycle control, nuclear factor (erythroid-derived 2)-like 2 (NRF2)–mediated oxidative stress responses, lipid metabolism, glutathione metabolism, oxidative phosphorylation, and signal transduction. Furthermore, Ingenuity Pathway and bioinformatic analyses revealed that expression changes of genes encoding proteins with altered expression detected in GST-P+ foci are likely to be controlled by c-myc, NRF2, aryl hydrocarbon receptor, nuclear factor kappa B, and hepatocyte nuclear factor 4 transcriptional factors. Co-ordinated overexpression of mitochondrial chaperons prohibitin (PHB) and prohibitin 2 (PHB2), septin 9 (SEPT9), neurabin 1, and other cytoskeletal and functional proteins in areas of GST-P+ foci during initiation and/or promotion stages of rat hepatocarcinogenesis was associated with induction of cell proliferation and might be responsible for the neoplastic transformation of rat liver preneoplastic lesions. Newly discovered elevation of PHB, PHB2, and SEPT9 in GST-P+ foci and tumors, imply that they might play important role in the onset of liver cancer and be of potential values in the studies of hepatocarcinogenesis.

Key Words: GST-P–positive foci; proteomics; hepatocarcinogenesis.

It is now accepted that the understanding of carcinogenesis and tumor progression on a molecular basis needs detailed study of proteins as critical components and effector molecules of the multiple interconnected signaling pathways that drive the neoplastic phenotype. However, investigations of the proteomes of small tissue samples preneoplastic or neoplastic lesions have remained limited mostly because of technological difficulties, and new approaches need to be developed.

At present, the molecular mechanisms of development and progression of hepatocellular carcinoma (HCC) are not well understood (Seow et al., 2000). High-throughput, proteomic techniques targeting biological molecules may provide novel insights into hepatocarcinogenesis and prognosis (Melle et al., 2004). In rat hepatocarcinogenesis, glutathione S-transferase placental form positive (GST-P+) foci arise after initiation and are believed to reflect the later formation of tumors (Ito et al., 1992). However, not all of GST-P+ foci which might be observed in the rat liver are finally developed into liver adenomas and carcinomas. Furthermore, the sequence of events and mechanisms of hepatocarcinogenesis remain unclear. We have recently demonstrated significant overexpression of cytokeratin (CK) 8 and CK18 in rat liver GST-P+ foci as well as mouse basophilic foci using surface-enhanced laser desorption/ionization time-of-flight mass spectrometry Protein-Chip arrays (Kakehashi et al., 2009, 2010). Elevation of CK8/18, and formation of these two CK complex associated with histone type 2 H2aa3 upregulation and intermediate filament reorganization, was shown to drive neoplastic transformation of preneoplastic lesions in the rat and mouse liver leading to formation of HCCs. To study further mechanisms of hepatocarcinogenesis and to develop a platform for proteomic analysis of small preneoplastic lesions which might be applied in multiple basic science areas, we here performed an analysis of microdissected GST-P+ foci using the QSTAR Elite liquid chromatography with tandem mass spectrometry (LC-MS/MS) system allowing multiple protein identification (Gluckmann et al., 2007). Furthermore, we applied iTRAQ isobaric reagents, which can be utilized in combination with liquid

chromatography with tandem mass spectrometry (LC-MS/MS) for multiplex protein profiling and quantification up to four different samples. Data obtained by LC-MS/MS were verified by immunohistochemistry and further analyzed by Bioinformatic and Ingenuity Pathway (IPA) analyses.

MATERIALS AND METHODS

Chemicals. N-nitrosodiethylamine (DEN) was from Sakai Research Laboratory (Fukui, Japan). Phenobarbital (PB) sodium salt (CAS no. 57-30-7) (purity ≥ 98%) and other reagents were purchased from Wako Pure Chemicals Industries or Sigma (St Louis, MO).

Animals. A total of 60, 5-week-old male Fisher 344 rats (Charles River, Japan, Hino, Shiga, Japan) were quarantined for 1 week before the start of the experiment. They were housed in an animal facility maintained on a 12 h (7:00–19:00) light/dark cycle, at a constant temperature of 23°C ± 1°C and relative humidity of 44 ± 5% and were given free access to tap water and food (Oriental MF pellet diet, Oriental Yeast Co., Tokyo, Japan). All experimental procedures were conducted following approval of the Animal Care and Use Committee of the Osaka City University Medical School.

Experimental design. Sixty F344 rats were divided into two experimental groups. After 1 week on basal diet, all animals underwent intraperitoneal injection of DEN (100 mg/kg body weight) dissolved in saline to initiate hepatocarcinogenesis. This was performed three times, once per week. After one further week on basal MF diet, animals were administered diet containing PB at a dose of 0 (control) or 500 ppm for 10 (10 rats per group) or 33 (20 rats per group) weeks. At experimental weeks 13 and 36, terminations were performed. The time points for terminations were selected based on Solt-Farber protocol to compare the development of rat liver preneoplastic lesions (GST-P⁺ foci) and liver tumors as well as their proteomes with adjacent normal-appearing liver tissues.

At week 13, liver perfusion was performed as described previously (Kinoshita *et al.*, 2002). Liver tissue frozen fixation in optimal cutting temperature (OCT) compound with isopentane was prepared for the QSTAR Elite LC-MS/MS (AB Sciex, Concord, ON, Canada). Liver tumors at 36 weeks were fixed with OCT compound for proteome analysis and 10% formalin for the histological examination.

Immunohistochemical staining of GST-P⁺ foci and their laser microdissection. Immunohistochemical demonstration of GST-P⁺ foci and Hematoxylin and Eosin (HE) staining for assessment of the incidence, multiplicity, and histopathological classification of liver tumors were carried out at weeks 13 and 36, respectively (Kitano *et al.*, 1998). For laser microdissection, GST-P⁺ foci were identified by staining in frozen sections and dissected as described previously (Kakehashi *et al.*, 2009). For QSTAR LC-MS/MS, samples from approximately 75,000 cells = (~1,250,00,000 µm² area) of GST-P⁻ foci, HCCs and normal-appearing liver in 50 µl of 9M urea/2% 3-[(3-cholamidopropyl)dimethylammonio]-1-propanesulfonate lysis buffer were prepared. Normal-appearing surrounding liver tissue was microdissected from the rats harboring GST-P⁺ foci and pulled samples were prepared. The representative pictures of microdissected GST-P⁺ foci and normal-appearing liver tissue are shown in Figure 3.

QSTAR Elite Hybrid LC-MS/MS. Proteome analysis was performed on a DiNa-AI nano LC System (KYA Technologies, Tokyo, Japan) coupled to a QSTAR Elite hybrid mass spectrometer (AB Sciex) through a NanoSpray ion source (AB Sciex). Mobile phase A was 98% water (2% acetonitrile [ACN], 0.1% formic acid), and mobile phase B was 70% ACN (0.1% formic acid, 30% water). The column effluent was introduced into the spray chamber through a tapered stainless steel emitter and directly electrosprayed into the QSTAR System ion trap mass spectrometer in the positive mode for nanoESI-MS/MS analysis. One sample was run for 150 min.

iTRAQ labeling and quantification of protein expression. Protein lysates from microdissected GST-P⁺ foci and HCCs and normal-appearing areas from

the liver of rats treated with DEN followed by PB at doses of 0 and 500 ppm were digested and labeled with 4-plex iTRAQ reagents according to standard procedures (Glückmann *et al.*, 2007). The samples were labeled as described below: 114, normal-appearing liver area in DEN → PB-treated groups (13 or 36 weeks); 115, GST-P⁺ foci or HCCs in DEN → PB-treated groups; 116, normal-appearing liver area in DEN initiation control groups (13 or 36 weeks); 117, GST-P⁺ foci and HCCs in the DEN initiation control groups. Each sample contained 30 µg protein. Protein concentrations were measured with BCA Protein Assay Kit (Pierce, IL).

IPA and bioinformatic analyses. The Ingenuity program (Ingenuity Systems, Mountain View, CA) was utilized to identify networks of interacting proteins, functional groups, and pathways. Bioinformatic analysis of gene promoters encoding proteins with altered expression was performed using PROMOSER and TFSEARCH internet databases for identification of common transcriptional factors that may be driving the expression changes. Identified transcriptional factors localization was further examined by immunohistochemistry.

Validation of protein expression by immunohistochemistry. Differentially expressed proteins in GST-P⁺ foci of rats treated with DEN and PB were verified by single and double immunohistochemistry. Paraffin sections containing normal liver tissue and GST-P⁺ foci were used for comparison and stained using standard immunohistochemical methods. For this purpose, we generated new monoclonal mouse anti-rat CK8 and CK18 antibodies, rat monoclonal prohibitin (PHB), prohibitin 2 (PHB2), and septin 9 (SEPT9) antibodies using the rat lymph node method (all from Risk Assessment and Research, Inc., Japan) (Tachibana *et al.*, 2010). Furthermore, guinea pig polyclonal antibodies against CK8 and 18 (Progen Biotechnik, Germany), monoclonal anti-histone H2A (H2aa3) antibody (Upstate Biotechnology, Inc.), goat polyclonal antibodies against neurabin 1, mucin 2, microsomal glutathione S-transferase 1 (MGST1), apolipoprotein A1 (APOA1), apolipoprotein E (APOE), alpha-2-macroglobulin (A2M), CK13, and CK14 (Santa Cruz Biotechnology), guinea pig polyclonal CK17 antibody (Progen Biotechnik), rabbit polyclonal CK5 antibody (Abcam Co., Japan), rabbit polyclonal antibodies against progesterone receptor and cytochrome b5 (Santa Cruz Biotechnology), goat polyclonal epoxide hydrolase 1 antibodies (Abcam Co., Japan), rabbit polyclonal uridine diphosphate (UDP)-glucose pyrophosphorylase 2 antibody (UGP2; Protein Tech Group, Inc.), c-myc and nuclear factor (erythroid-derived 2)-like 2 (NRF-2) rabbit polyclonal antibodies (Abcam Co.), aryl hydrocarbon receptor (AhR) mouse monoclonal antibodies (Abcam Co.), and hepatocyte nuclear factor 4 (HNF-4) rabbit polyclonal antibody (Bioworld Technology, Inc.) were employed for clarification of the results. Immunohistochemical procedure was optimized by testing different antigen retrieval methods and negative controls.

Statistical analysis. For analysis of protein expression, statistical analysis with ProteinPilot 2.0 Software was employed. The significance of differences between mean values was analyzed by the *t*-test using the StatLight-2000(C) program (Yukms Corp., Japan).

RESULTS

GST-P⁺ Foci and Histological Examination of Liver Tumors

After 10 weeks of continuous PB administration to rats followed DEN initiation, significant increase in number and area of GST-P⁺ foci was found in the group treated with PB at a dose of 500 ppm (161.91 ± 36.59 no./cm², $p < 0.001$; 3.08 ± 0.92 mm²/cm², $p < 0.0001$) as compared with the DEN initiation control group (128.04 ± 16.51 no./cm²; 1.41 ± 0.54 mm²/cm²). Histological examination of liver tumors at week 36 demonstrated a significant induction of HCC (9.60 ± 3.15 no./rat,

$p < 0.0001$) and total tumors (13.7 ± 3.53 no./rat, $p < 0.0001$) multiplicities in the group treated with PB at 500 ppm as compared with the DEN initiation control group (HCC: 3.00 ± 1.95 no./rat and total tumors: 6.65 ± 2.64 no./rat). Most tumors developing in animals administered 500 ppm of PB were well-differentiated HCCs. Hepatocytes hypertrophy and slight fatty changes were observed in the normal-appearing liver tissue of rats treated with DEN and PB.

Alteration of Protein Expression in Rat Liver GST-P⁺ Foci

The results of the QSTAR Elite LC-MS/MS and IPA analyses of the GST-P⁺ foci of rats 13 weeks after initiation with DEN or DEN followed by 10 weeks treatment with PB at a dose of 500 ppm are presented in Tables 1 and 2 respectively. From microdissected GST-P⁺ foci and normal-appearing liver of rats in the initiation control and DEN followed by PB treatment groups, 75 proteins were identified with 95% confidence or higher and quantified using ProteinPilot 2.0 Software. In the GST-P⁺ foci of DEN-initiated animals, elevation of expression of 15 proteins and suppression of 12 proteins as compared with the adjacent normal-appearing tissue were detected. On the other hand, in the PB promotion group, in GST-P⁺ foci expression of 38 proteins was increased and of 12 was inhibited. Comparative analysis of overexpressed proteins (Venn diagram) in rat liver GST-P⁺ foci and results of analysis of protein subclasses and in DEN initiation control and PB promotion groups 13 weeks after DEN initiation detected by IPA are presented in Figures 1A and 1B. Hepatocarcinogenesis by DEN was associated with over-expression of mitochondrial chaperones and regulators of transcription PHB and PHB2, cellular transporters APOE and APOA1 regulating lipid metabolism, vimentin (VIM), proteins related to control of xenobiotic metabolism (MGST1, glutathione S-transferase M1 [GSTM1], glutathione S-transferase A1 [GSTA1], microsomal cytochrome b5 type A [CYB5A], and UGP2) and enzymes involved in oxidative phosphorylation (cytochrome C oxidase Vic [COX6C] α [ATP5A1], β [ATP5B], and δ [ATP5D] subunits of F1 mitochondrial complex of ATP synthases) as well as underexpression of fatty acid–binding protein 1 (FABP1) and enzymes of the urea cycle (carbamoyl-phosphate synthetase 1 [CPS1], ornithine carba-moyltransferase [OTC], and argininosuccinate synthase 1 [ASS1]) in the area of GST-P⁺ foci (Table 1 and Fig. 1A). Furthermore, elevation of SEPT9, central nervous system (CNS) protein neurabin 1 (Neb1), cyclin B3 (CCNB3), intermediate filaments CK5, CK8, CK13, CK14, CK17, and CK18, progesterone receptor membrane component 1 (PGRMC1), histone H2A type 1 (H2aa3) and histone H2B type 1 (H2be), transporter A2M, chaperones heat shock 10-kDa protein 1 (chaperonin 10) (HSPE1) and protein disulfide isomerase A3 (PDIA3), glutathione S-transferase M5 (GSTM5) and suppression of detoxification enzymes (catalase [CAT] and paraoxonase 1 [PON1]) and L-tyrosine catabolizing enzyme 4-hydroxyphenylpyruvate dioxygenase [HPD] were associated

with promotion of rat hepatocarcinogenesis by PB (Table 2 and Fig. 1A). As compared with the GST-P⁺ foci protein spectrum of the DEN control livers, in preneoplastic lesions of PB promotion group, a significant number of proteins with increased expression participated in NRF2-mediated oxidative stress response, glutathione metabolism, lipopolysaccharides/ interleukin-1–mediated inhibition of RXR function, xenobiotic metabolism, AhR signaling, and cellular assembly and organization pathways (Fig. 1B). SEPT9 and Neb1 were indicated by IPA likely to be involved in Rho-dependent organization of F-actin.

IPA and Bioinformatic analyses of the promoter regions of genes encoding proteins with altered expression in GST-P⁺ foci of initiation and promotion groups have demonstrated that common transcriptional factors which may be driving the expression changes are c-myc, NRF2, nuclear factor kappa B (NF-κB), HNF-4, and AhR. Most of differentially expressed proteins detected by QSTAR Elite MS/MS were targets for these transcriptional factors and contained binding sites. Thus, PHB, PHB2, SEPT9, and Neb1 are likely to be controlled by c-myc, NRF2, and NF-κB (data not shown). On the other hand, PHB, PHB2, PGRMC1, H2aa3, MGST1 and downregulated enzymes of urea cycle; HPD and FABP might be regulated by HNF-4 (Fig. 2 and data not shown).

Additionally, we have compared the proteomes of the adjacent normal-appearing liver tissues of rats treated with DEN alone and DEN followed by PB. PB treatment resulted in increase of phase I and phase II metabolizing enzymes including CYB5A, UGP2 and MGST1, EPHX1, COX6C, APOE, APOA1, VIM, CK5, CK8 in the normal-appearing tissue (data not shown). However, no alterations in expression of mitochondrial prohibitins, SEPT9, Neb1, PGRMC1, H2aa3, H2be, CCNB3, A2M, and other proteins detected by proteome analysis of GST-P⁺ foci were found indicating that observed changes do not occur in normal-appearing liver tissue.

Comparison of Alterations of Protein Expression in Preneoplastic Lesions and HCCs Detected by QSTAR Elite LC-MS/MS

Similar to the GST-P⁺ foci, in the HCCs of initiation control and PB-promoted rat livers 36 weeks after DEN initiation, upregulation of PHB and PHB2, SEPT9, Neb1, APOE, intermediate filaments proteins CK8, CK18, and VIM, was found compared with the adjacent normal-appearing liver tissue (data not shown). Inhibition of CAT, PON1, FABP1, and enzymes participating in urea cycle, CPS1, OTC, and ASS1, was detected in HCCs, again to that observed for GST-P⁺ foci (data not shown). Furthermore, in HCCs, promotion by PB was associated with significant elevation of phase II metabolizing enzymes such as GST 7-7, GSTA4, GSTA2, GSTM1, and CK5. Induction of CK19, annexin A1, and annexin A5 was observed in HCCs of rats administered DEN alone or DEN

TABLE 1

Differentially Expressed Proteins in the Liver GST-P$^+$ Foci of Rats 13 Weeks after DEN Initiation, Identified by QSTAR Elite LC-MS/MS

Protein	GI number	Mass (Da)	Location	Family	Function	Fold change	P
UDP-glucose pyrophosphorylase 2 (UGP2)	67078526	57024	C	E	XM	1.54	0.0003
Glutathione S-transferase A1 (GSTA1)	13928688	25320	C	E	XM	1.43	0.0000
Cytochrome b5 type A (microsomal) (CYB5A)*	11560046	15355	C	E	XM	1.22	0.0000
Microsomal glutathione S-transferase 1 (MGST1)	19705453	17472	C	E	XM	0.64	0.047
Glutathione S-transferase M1 (GSTM1)*	28933457	25703	C	E	XM	0.64	0.0001
Vimentin (VIM)*	14389299	53733	C	O	CS	1.86	0.022
Collagen, type I, alpha 1 (COL1A1)	27688933	25320	ES	O	CS	1.44	0.021
Cytochrome c oxidase, subunit VIc (COX6C)	9506509	7317	C	E	OP	2.01	0.001
ATP synthase, H+ transporting, mitochondrial F1 complex, α subunit 1 (ATP5A1)	40538742	59754	C	T	OP, T	1.35	0.000
ATP synthase, H+ transporting, mitochondrial F1 complex, δ subunit (ATP5D)	20806153	17595	C	T	OP, T	1.23	0.0005
ATP synthase, H+ transporting, mitochondrial F1 complex, β polypeptide (ATP5B)	54792127	56354	C	T	OP, T	1.14	0.0000
ATP synthase, H+ transporting, mitochondrial F0 complex, subunit δ (ATP5H)	9506411	18764	PM	T	OP, T	0.84	0.0068
Ornithine carbamoyltransferase (OTC)*	6981312	39887	C	E	M	0.84	0.02
Acetyl-coenzyme A acyltransferase 2 (ACAA2)	18426866	41871	C	E	M	0.82	0.019
Glyceraldehyde-3-phosphate dehydrogenase (GAPDH)	8393418	35828	C	E	M	0.76	0.0055
Aldehyde dehydrogenase 2 family, mitochondrial (ALDH2)	14192933	56489	C	E	M	0.7	0.0001
Enoyl coenzyme A hydratase, short chain, 1, mitochondrial (ECHS1)	17530977	31517	C	E	M	0.68	0.021
Argininosuccinate synthetase 1 (ASS1)*	25453414	46497	C	E	M	0.07	0.0001
Carbamoyl-phosphate synthetase 1, mitochondrial (CPS1)*	8393186	164582	C	E	M	0.52	0.0000
Prohibitin (PHB)*	13937353	29820	N, Mi	TR	TR	1.5	0.0001
Prohibitin 2 (PHB2)*	61556754	33312	N, Mi	TR	TR	2.34	0.0002
Heat shock 70-kDa protein 5 (HSPA5)	25742763	72348	C	O	HSP	1.32	0.0000
DnaJ (Hsp40) homolog, subfamily B, membrane 11 (DNAJB11)	62543491	40496	C	O	HSP	1.19	0.0225
Heat shock 60-kDa protein 1 (chaperonin) (HSPD1)	11560024	60966	C	O	HSP	0.85	0.003
Cytoplasmic polyadenylation element binding protein 2 (CPEB2)	109499825	96462	U	O	O	1.44	0.0335
Apolipoprotein E (APOE)*	20301954	36038	ES	T	T	1.40	0.0001
Apolipoprotein A1 (APOA1)*	146345369	30062	ES	T	T	1.61	0.001
Fatty acid–binding protein 1, liver (FABP1)*	6978825	14273	C	T	LM	0.68	0.0000

Note. C, cytoplasm; N, nucleus; PM, plasma membrane; ES, extracellular space; Mi, mitochondria; CS, cytoskeleton; TR, transcriptional regulator; CC, cell cycle; E, enzyme; T, transporter; K, kinase; Ph, phosphatase; OP, oxidative phosphorylation; IC, ion channel; A, adhesion; D, detoxification; XM, xenobiotic metabolism; M, metabolism; LM, lipid metabolism; HSP, heat shock protein; CNS, protein of the CNS; R, receptor; ISP, intestinal secreted protein; U, unknown; O, other; "*" denotes that same changes of protein expression were observed in HCCs.

followed by PB. In addition, in HCCs of rats in both groups expression of detoxification enzymes glutathione peroxidase 1 (GPx-1) and superoxide dismutase 1 (SOD1) was suppressed as compared with the normal liver tissue (data not shown).

Validation of Protein Expression Findings by Immunohistochemistry

Differential expression of proteins in GST-P$^+$ foci and tumors of DEN control and PB-administered animals 13 and

TABLE 2

Differentially Expressed Proteins in the Liver GST-P$^+$ Foci of Rats Treated with DEN Followed by 10 Weeks on PB at a Dose of 500 ppm, Identified by QSTAR LC-MS/MS

Protein	GI number	Mass (Da)	Location	Family	Function	Fold change	P
Microsomal glutathione S-transferase 1 (MGST1)	19705453	17472	C	E	XM	3.21	0.0467
Epoxide hydrolase 1, microsomal (xenobiotic) (EPHX1)*	77539448	52582	C	P	XM	2.23	0.0500
Esterase 22 (ES22)	2494387	62495	C	E	XM	2.03	0.0400
Glutathione S-transferase M5 (GSTM5)	8393502	25914	C	E	XM	1.87	0.0400
Glutathione S-transferase A3 (GSTA3)	232203	25361	C	E	XM	1.7	0.0398
Glutathione S-transferase A1 (GSTA1)	1170084	25319	C	E	XM	1.52	0.0500
Glutathione S-transferase A4 (GSTA4)*	109478305	25510	C	E	XM	1.39	0.0500
Glutathione S-transferase M1 (GSTM1)*	28933457	25703	C	E	XM	1.39	0.0500
Cytochrome b5 type A (microsomal) (CYB5A)*	11560046	15199	C	E	XM	1.25	0.0000
UDP-glucose pyrophosphorylase 2 (UGP2)	67078526	57024	C	E	XM	1.13	0.0395
Cytochrome P450, 2A12 (CYP2A12)	3913322	56345	C	E	XM	0.95	0.0119
Cytokeratin 17 (CK17)*	23396626	48162	C	O	CS	2.18	0.0412
Type I keratin KA11 (Ka11)	57012432	52596	U	O	CS	2.17	0.0500
Cytokeratin 14 (CK14)*	81170667	52684	C	O	CS	1.92	0.0436
Cytokeratin 13 (CK13)*	51591909	47729	C	O	CS	1.62	0.0400
Cytokeratin 5 (CK5)*	50233797	61928	C	O	CS	1.49	0.0073
Cytokeratin 18 (CK18)*	68534953	47761	C	O	CS	1.32	0.0001
Cytokeratin 76 (CK76)	57012372	61758	U	O	CS	1.31	0.0173
Cytokeratin 8 (CK8)*	40786432	54019	C	K	CS	1.17	0.0100
Cytochrome c oxidase, subunit VIc (COX6C)	9506509	7317	C	E	OP	1.5	0.0007
ATP synthase, H+ transporting, mitochondrial F0 complex, subunit E (ATP5I)	17978459	8255	C	T	OP,T	1.25	0.0342
ATP synthase, H+ transporting, mitochondrial F1 complex, δ subunit (ATP5D)	20806153	17595	C	T	OP,T	1.19	0.0073
ATP synthase, H+ transporting, mitochondrial F1 complex, β polypeptide (ATP5B)	54792127	56354	C	T	OP,T	1.07	0.0077
Protein disulfide isomerase family A, member 3 (PDIA3)	8393322	56590	C	P	P	1.14	0.0247
Mast cell protease 8-like 2 (RGD: 1302938)	109502449	34849	U	P	P	0.52	0.0000
4-Hydroxyphenylpyruvate dioxygenase (HPD)	8393557	45113	C	E	M	0.79	0.0044
Ornithine carbamoyltransferase (OTC)*	6981312	39886	C	E	M	0.78	0.0011
Carbamoyl-phosphate synthetase 1, mitochondrial (CPS1)*	8393186	164580	C	E	M	0.62	0.0003
Malate dehydrogenase 1, NAD (soluble) (MDH1)	15100179	36483	C	E	M	0.69	0.0001
Histone H2B type 1 (histone cluster 2, H2be)*	399856	13859	N	TR	TR	1.35	0.045
Histone H2A type 1 (histone cluster 2, H2aa3)*	90101451	13964	N	TR	TR	1.22	0.0004
Prohibitin (PHB)*	13937353	29820	N,Mi	TR	TR	1.23	0.0004
Prohibitin 2 (PHB2)*	76363296	33312	N,Mi	TR	TR	1.25	0.04
Bromodomain adjacent to zinc finger domain, 2B (BAZ2B)	109469903	241350	U	O	TR	0.88	0.0100
Septin 9 (SEPT9)*	28849875	63793	C	E	CC	1.82	0.0000
Cyclin B3 (CCNB3)	109511595	45190	N	O	CC	1.24	0.0063
Transmembrane protein 142A (ORAI1)	81883090	33040	U	IC	IC	1.24	0.0035
Potassium voltage-gated channel, member 5 (KCNQ5)	109486878	102312	PM	IC	IC	0.81	0.0012
Catalase (CAT)*	6978607	59757	C	E	D	0.57	0.0150

TABLE 2—Continued

Protein	GI number	Mass (Da)	Location	Family	Function	Fold change	P
Paraoxonase 1 (PON1)*	54292130	39358	ES	E	D	0.09	0.0174
Similar to precursor of mucin 2 (MUC2)	109482915	166038	ES	O	ISP	3.21	0.0060
Progesterone receptor membrane component 1 (PGRMC1)*	11120720	21598	PM	O	R	1.61	0.0028
Alpha-2-macroglobulin (A2M)*	6978425	163785	ES	T	PI	1.38	0.0500
Protein phosphatase 1, inhibitor subunit 9A (Neb1)*	13431726	122735	C	CNS	ABP	1.4	0.0038
Heat shock 10-kDa protein 1 (chaperonin 10) (HSPE1)	6981052	10876	C	E	HSP	1.42	0.0309
Cell adhesion molecule 4 (CADM4)	114052915	42781	PM	O	A	1.32	0.0474
Apolipoprotein E (APOE)*	20301954	36038	ES	T	T	1.12	0.0056
Apolipoprotein A1 (APOA1)*	146345369	30062	ES	T	T	1.80	0.001
Olfactory receptor 585 (OLFR585)	47606357	35570	PM	G-pro	G-pro	0.82	0.0380
Fatty acid–binding protein 1, liver (FABP1)*	6978825	14273	C	T	LM	0.71	0.0220

Note. C, cytoplasm; N, nucleus; PM, plasma membrane; ES, extracellular space; Mi, mitochondria; CS, cytoskeleton; TR, transcriptional regulator; CC, cell cycle; E, enzyme; R, receptor; T, transporter; K, kinase; Ph, phosphatase; OP, oxidative phosphorylation; IC, ion channel; A, adhesion; D, detoxification; XM, xenobiotic metabolism; M, metabolism; LM, lipid metabolism; HSP, heat shock protein; CNS, protein of the CNS; ISP, intestinal secreted protein; P, peptidase; G-pro, G-protein–coupled receptor; PI, proteinase inhibitor; ABP, actin-binding protein; RBP, RNA-binding protein; U, unknown; O, other; "*" denotes that same changes of protein expression were observed in HCCs.

36 weeks after initiation, respectively, was verified by single and double immunohistochemistry. In Figure 3, representative pictures of HE staining and immunohistochemical (IHC) findings for PHB, PHB2, SEPT9, Neb1, APOE, A2M, and PCNA and double> staining for GST-P and CK8/18 in serial sections of GST-P⁺ foci and HCC of the rat from the promotion group are presented (Figs. 3A and 3B). Interestingly, in several large size GST-P⁺ foci, overexpression of PHB2, PHB, SEPT9, Neb1, PGRMC1, APOE, APOA1, A2M, CK8/CK18, CK13, CK14, CK17, and cell proliferation marker PCNA was observed (Fig. 3A and data not shown). Expression within areas of GST-P⁺ foci appeared coordinated, although staining intensity varied. Furthermore, all GST-P⁺ foci in livers of rats administered PB were positive for MUC2, EPHX1, UGP2, MGST1, and CYB5A (data not shown).

Significant overexpression of PHB2, PHB, SEPT9, APOE, APOA1, UGP2, CYB5A, MGST1, EPHX1, COX6C, CK8, CK18, and PCNA was found in the liver HCCs in initiation and/or promotion groups (Fig. 3B and data not shown). Mozaic staining in HCCs was observed for Neb1, A2M, CK13, CK14, and CK17. All hepatocellular adenomas (HCAs) were positive for GST-P, UGP2, CYB5A, MGST1, EPHX, and COX6C (data not shown). Furthermore, some HCAs were positive for PHB, PHB2, SEPT9, Neb1, PGRMC1, APOE, APOA1, A2M, MUC2, CK5, CK8, CK13, CK14, CK17, CK18, and PCNA (data not shown). In addition, in the normal-appearing liver area of both initiation control and PB-treated rat livers, overexpression of CK8, UGP2, CYB5A, MGST1, EPHX1, and COX6C was detected.

Immunohistochemical analysis of common transcriptional factors including c-myc, NRF2, AhR, and HNF4 which may be driving the expression changes of proteins detected by QSTAR Elite LC-MS/MS have demonstrated their induction in the area

of several large GST-P⁺ foci and HCCs (Fig. 3 and data not shown). C-myc was elevated in the cytoplasm, whereas NRF2, AhR, and HNF-4 were localized in both cytoplasm and nuclei of tumor cells.

DISCUSSION

In the present study, we identified GST-P⁺ foci protein profiles using QSTAR Elite LC-MS/MS which is able to detect minute amounts of proteins and moreover to analyse complex protein patterns. To our knowledge, this study provided the first experimental evidence for PHB, PHB2, and SEPT9 overexpression in rat liver preneoplastic lesions. Immunohistochemical examination supported the results of QSTAR Elite LC-MS/MS and furthermore demonstrated high concordance between induction of PHB, PHB2, SEPT9, Neb1, PGRMC1, APOE, APOA1, A2M, H2aa3, CK5, CK8, CK13, CK14, CK17, and CK18 in the same areas of several large size GST-P⁺ foci and HCCs. Furthermore, these protein overexpression appeared strongly associated with induction of cellular proliferation. IPA and Bioinformatic analyses of promoter regions of genes encoding these proteins have revealed that c-myc, NRF2, HNF-4, NF-κB, and AhR might be the common transcriptional factors which may be driving the expression changes of proteins in GST-P⁺ foci, thus suggesting their important role in control of rat hepatocarcinogenesis. PHB, PHB2, SEPT9, and Neb1 are likely to be controlled by c-myc, NRF2, and NF-κB. Furthermore, PHB, PHB2, PGRMC1, and H2aa3 are the possible targets for HNF-4.

Recently, NRF2 pathway, namely, its propensity to be hijacked by cancer cells where it facilitates a prosurvival phenotype has been shown (Malhotra *et al.*, 2010; Wakabayashi